4. MW-CHERENKOV COUNTER

In this chapter, I will first describe the main characteristics of a Cherenkov counter that determine its performance and then the MW-Cherenkov counter itself. Finally, I will describe how the MW-Cherenkov was used to tag the minority particles during the E706 run.

4.1. INTRODUCTION

Cherenkov radiation was discovered in 1943 by Vavilov and Cherenkov[58] and was explained theoretically by Tamm and Frank[59] in 1937 who developed a classical theory to account for the radiation. A quantum-mechanical theory of the effect was given by Ginsburg[60] in 1940.

The relation between the angle of Cherenkov radiation, θ, the velocity of the particle, β, and the refractive index of the medium, $\eta(\lambda)$, is:

$$\cos\theta = \frac{1}{\beta\eta(\lambda)} \tag{4.1}$$

Relation (4.1) can be rewritten as:

$$\cos\theta(\lambda) = \frac{v_{\text{light}}}{v_{\text{particle}}} \tag{4.2}$$

which shows that the angle of emission of light is directly related to the ratio of the

velocity of light in the radiator to the particle velocity. The optical measurement of the emission angle of the light, along with the knowledge of the velocity of light in the same medium, determines the velocity of a particle. For high-energy charged particles, measuring their relative velocity β via Cherenkov radiation together with an independent determination of their momenta p is practically the primary way to identify the particles.

By using the Cherenkov effect, the velocity can be measured to a percentage accuracy in the range of 10^{-3} to 10^{-7}, with the corresponding accuracy in mass, m, of a single particle given by:

$$dm/m = \gamma^2(d\beta/\beta) + (dp/p) \tag{4.3}$$

where dp/p is the momentum spread of the beamline. Due to the large γ^2 factor at high energies, the ability to identify particles by this mass definition is limited by the velocity resolution of the particular Cherenkov detector.

There are three basic types of Cherenkov detectors that are used for particle identification at high energies[61]:

a) *The threshold counter*, which is used to detect particles that have velocity β above a given threshold velocity β_0.

b) *The differential counter*, which distinguishes among different particles by the angle of their Cherenkov light. In a differential counter the reflected ring of Cherenkov light is focused into an annular diaphragm. The light that passes through the aperture of the diaphragm is detected by a number of photomultipliers equally spaced around the annulus.

c) *The differential isochronous self-collimating counter (DISC).* which is a differential counter equipped with an optical system which corrects for geometric and chromatic aberrations.

All three types of counters are illustrated schematically in Fig. 31.

In a high energy beam of momentum p the velocity resolution $\Delta\beta$ of a Cherenkov counter is defined in terms of the range of the Cherenkov angle accepted by the counter:

$$\Delta\beta = \tan\theta \ \Delta\theta \tag{4.4}$$

The approximate velocity difference $\Delta\beta_{m_0 m_1}$ between two particles with masses m_0, and m_1 and the same momentum is given by

$$\Delta\beta_{m_0 m_1} = \frac{(m_1^2 - m_0^2)}{2p^2}, \tag{4.5}$$

with $m_1 > m_0$.

The limiting mass separation of a Cherenkov counter corresponds to the finest velocity resolution $\Delta\beta_{limit}$ that the counter can achieve. For the limiting separation of two particles one must have:

$$\Delta\beta_{limit} = \Delta\beta_{m_0 m_1} \tag{4.5}$$

In practice, $\Delta\beta_{limit}$ is chosen so that

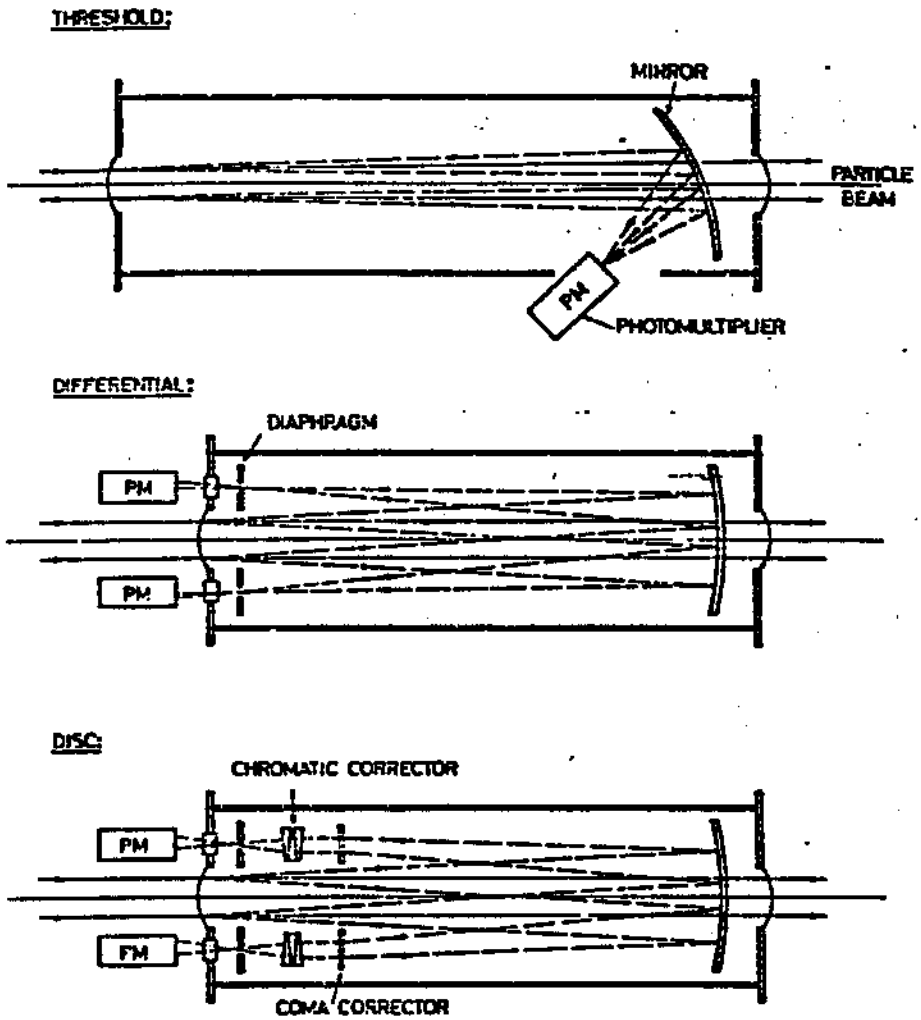

Figure 31: Basic Types of Cherenkov Detectors.

$$\Delta\beta_{limit} = \frac{1}{4}\Delta\beta_{m_0 m_1} \tag{4.6}$$

As a numerical example, the mass separation between pions and kaons at 300 GeV is $\Delta\beta_{m_0 m_1} \sim 10^{-6}$. To resolve between pions and kaons at this energy using a Cherenkov counter demands a small value for the Cherenkov angle from Eq. (4.4), and consequently a small value of the refraction index $(\eta - 1)$. Therefore at high energies one considers only gas-filled Cherenkov counters.

Before I go on to describe the MW Cherenkov counter I will discuss the main characteristics that determine the performance of a Cherenkov counter.

4.2. Performance Characteristics of a Cherenkov Counter

4.2.1 The light yield

The number of photons N per unit wavelength λ in a counter of finite length L is given by:

$$\frac{d^2N}{d\lambda d\cos\theta} = \frac{z^2 2\pi\alpha}{\lambda}\left(\frac{L}{\lambda}\right)^2\left(\frac{\sin\chi}{\chi}\right)^2\sin^2\theta, \tag{4.8}$$

where

$$\chi(\theta) = \pi\frac{L}{\lambda}\left(\frac{1}{\eta(\lambda)\beta} - \cos\theta\right), \tag{4.9}$$

ze is the charge of the particle, α is the fine structure constant and $\eta(\lambda)$ is the refraction index of the radiator.

In the limit $(L/\lambda \to \infty)$, $\sin\chi/\chi$ becomes a δ-function and

$$\frac{d^2N}{d\lambda\ d\cos\theta} = \frac{z^2 2\pi\alpha}{\lambda}\delta(\chi)\left(\frac{L}{\lambda}\right)^2\sin^2\theta \tag{4.10}$$

which, when the δ-function is integrated over all angles, reduces to:

$$\frac{dN}{d\lambda} = \frac{z^2 2\pi\alpha}{\lambda^2}L\sin^2\theta \tag{4.11}$$

Due to the z^2 dependence, a particle with a large charge can generate sufficient Cherenkov light intensity to be recorded on photographic emulsion. However, for

singly charged particles, the light yield is quite small. For example, the energy loss by Cherenkov radiation in the wavelength bandwidth from 200 to 600 nm is about $1keV$, which is about 100 times less than the energy loss by ionization.

As we see from Eq. (4.11), the light yield is proportional to the length of the radiator and increases with decreasing wavelengths. Thus, many efforts have been made to improve the light transmission and extend the sensitivity of the photodetector into the ultraviolet region where the number of photons is greater. At long wavelengths the detection by the counter is limited not only by the reduced Cherenkov light emission but also by the cut off threshold of the photomultiplier photocathodes.

4.2.2 Quantum Efficiency and Noise

The detection efficiency of a given Cherenkov counter is obtained by folding the quantum efficiency of the photodetector used with the optical transmission properties of the counter, both of which are a function the Cherenkov light spectrum. By using ultraviolet-transmitting materials such as fused silica, the Cherenkov light can be detected to wavelengths of about 150 nm.

The effective detector efficiency of a photodetector and its the associated electronic equipment can be measured if one knows the bandwidth to be transmitted by the standard Cherenkov optics. The standard Cherenkov optics are those that are used in conventional threshold counters and consist of: (a) one front-aluminized mirror, especially coated for reflection at ultraviolet wavelengths and containing a

protective interference layer of $\lambda/2$ thickness of MgF_2 at 350 nm, and (b) one exit window of ultraviolet-transmitting fused silica which has an antireflection coating of a layer of $\lambda/4$ thickness of MgF_2 at 350 nm. With this standard set of Cherenkov optics it is possible to experimentally measure and compare the performances of different types of photomultipliers.

For a Cherenkov counter of length L and Cherenkov angle θ, the number of photoelectrons N produced by the passage of a single charged high-energy particle is given by:

$$N = AL\theta^2 \tag{4.12}$$

where A characterizes the photodetector, taking into account the Cherenkov light spectrum and the transmission properties of the optics. Values of the parameter A have been measured in several laboratories[62], and are in good agreement. The most sensitive photomultipliers available today, consisting of fused silica entrance window and a bialcali (K-Cs-Sb) photocathode, have a value of the parameter A from about 100-150 cm^{-1}. Photomultipliers having a photocathode of lower quantum efficiency and a UV-glass entrance window have a value of A from 50-60 cm^{-1}. For example, if L=42.1 m, θ=5.0 mrad and A = 150 cm^{-1} then Eq. (4.12) gives:

N = 16 Photoelectrons/particle

The noise pulses in a photomultiplier, mainly arising from single photoelectrons, are indistinguishable from true signals since the threshold of the detection electronics is generally set below that level. To avoid counting noise, in the differential type of Cherenkov counter, the light output is divided among several photomulti-

pliers, and their output signals required to satisfy a coincidence requirement. In this way the accidental count rate can be reduced to an extremely low level at the expense of reducing the overall counting efficiency of the detector.

For a differential Cherenkov counter with q photomultipliers, the efficiency for the q-fold coincidence is:

$$\epsilon_q = (1 - e^{-N/q})^q \tag{4.13}$$

where N is the number of photoelectrons.

For example, when q=6, $\epsilon_6 = 0.64$ for N=16 photoelectrons.

4.2.3 Optical Dispersion in the Radiator

In Eq. (4.1), the Cherenkov angle θ is a function of the wavelength λ of the light due to variation of the refractive index of the radiator as a function of λ. As a consequence, there is a spread or dispersion in the angle of the emitted photons due to variation of the refractive index of the radiator as a function of λ. The range of the chromatic dispersion is given by:

$$\Delta\theta_{DISP} = \frac{\Delta\eta}{\eta(\lambda)\tan\theta(\lambda)} \tag{4.14}$$

where $\Delta\eta$ is the change in refractive index over the range of the detectable wavelengths. If one defines an average wavelength λ_2 (which is the mean of the dis-

tribution of detected photoelectrons versus wavelength), and wavelengths λ_1, λ_3 corresponding to the limits of the spectral range, then

$$\Delta\theta_{DISP} = \frac{\eta(\lambda_2) - 1}{\eta(\lambda_2)\nu \tan\theta(\lambda_2)} \tag{4.15}$$

where

$$\nu = \frac{\eta(\lambda_2) - 1}{\eta(\lambda_1) - \eta(\lambda_3)} \tag{4.16}$$

The parameter ν characterizes the optical dispersion in the radiator. Table 6 contains values of the refractive index (at 1 atm and 20°C) and of the parameter ν for some commonly used gas radiators for wavelengths consistent with fused silica optics and the spectral response of a bialcali photocathode ($\lambda_1 = 280$ nm, $\lambda_2 = 350$ nm, $\lambda_3 = 440$ nm). As it is clear from the table, the inert gases have the largest values of ν and consequently the smallest chromatic dispersion.

TABLE 6				
Gas	$(n_0 - 1) * 10^6$ **[280 nm]**	$(n_0 - 1) * 10^6$ **[350 nm]**	$(n_0 - 1) * 10^6$ **[440 nm]**	ν
He	33.27	32.90	32.67	54.5
Ne	64.07	63.37	62.85	52.2
H_2	140.6	135.3	132.0	15.7
N_2	294.8	287.0	282.0	22.5
CH_4	447.8	430.3	419.7	15.3

TABLE 6: Values of the parameter ν for some commonly used gas radiators.

A precise expression for the refractive index of inert gases as a function of

wavelength at $0°C$ and 760 mm Hg was obtained by Dalgano and Kingston[66]. This useful expression for He is:

$$\eta^2 - 1 = 6.927 * 10^{-5}\left(1 + \frac{2.24 * 10^5}{\lambda^2} - \frac{5.94 * 10^{10}}{\lambda^4} - \frac{1.72 * 10^{16}}{\lambda^6} - ...\right) \quad (4.17)$$

4.2.4 Optical Aberrations

Most differential Cherenkov counters use a spherical mirrors to reflect and focus the Cherenkov light onto an annular diaphragm.

In a differential counter, a spherical mirror of radius of curvature R and focal length $f(= R/2)$ focuses the cone of Cherenkov light in the differential counter into a ring image of radius r, given by:

$$r = f \tan\theta \quad (4.18)$$

The total radial spread Δr of the ring image is determined by the spherical and coma aberrations which to the third order, are given by:

$$\Delta r = \frac{-1}{8}\left(\frac{d}{f}\right)^3 + \frac{1}{8}\left(\frac{d}{f}\right)^2\theta \quad (4.19)$$

In this expression the first term is the spherical error, the second is the coma, d is the useful diameter of the mirror, f is the focal length and θ is the Cherenkov angle.

Thus, the angular broadening $\Delta\theta_{OPT}$ of the ring image due to the optical aberrations is given by:

$$\Delta\theta_{OPT} = \frac{\Delta r}{f} \tag{4.20}$$

4.2.5 Energy Loss, Scattering, and Diffraction Effects

As the particle traverses the radiator it loses energy, primarily by the process of ionization, which changes the value of its velocity β and hence the Cherenkov angle of the radiated light. However, the ionization loss, which is about $2\text{MeV}^*\text{g}^{-1}*\text{cm}^{-2}$ for most materials, is negligible at relativistic energies. Multiple Coulomb scattering of the particle also causes a broadening of the Cherenkov angle. The angular spread $\Delta\theta_{MSC}$ (root mean squared projected angle) due to multiple scattering of a particle with momentum p can be expressed as[68]:

$$\Delta\theta_{MSC} = \left(\frac{14.1\ \text{Mev}}{p\beta}\right)\sqrt{\frac{L}{L_R}}\left[1 + \frac{1}{2}\log\left(\frac{L}{L_R}\right)\right] \tag{4.21}$$

where L is the radiator length and L_R its radiation length. For a gas radiator of length L, Eq.(4.21) can be rewritten as

$$\Delta\theta_{MSC} = \left(\frac{14.1\ \text{Mev}/c}{p\beta}\right)\left[\frac{\rho L(\eta - 1)}{(\eta_0 - 1)L_R}\right]^{\frac{1}{2}}, \tag{4.22}$$

where ρ is the gas density, L_R is the radiation length, η_0 is the refractive index

of the gas for a given wavelength of light at the temperature of the counter and pressure of 1 atm, and η is the refractive index at the same wavelength at the temperature and pressure of the counter.

The broadening of the Cherenkov angle $\Delta\theta_{DIFF}$ by diffraction is approximately given by:

$$\Delta\theta_{DIFF} = \frac{\lambda}{(L \sin\theta)} \tag{4.23}$$

where λ is the wavelength of light, L is the length of the radiator and θ is the Cherenkov angle. Since the gas-filled counters used to identify individual particles at ultra high energies operate at Cherenkov angles from 5 to 10 milliradians and are made tens of meters long (in order to obtain sufficient light) diffraction effects are negligible. For example the diffraction broadening for a 42.1 m long counter with θ=5 mrad and λ=350 nm is:

$$\Delta\theta_{DIFF} = 1.66 * 10^{-6} rads = 1.66 \mu rads$$

4.2.6 Finite Momentum Bite

Usually the beamlines where the Cherenkov counters are located are not monochromatic. The angular broadening of the Cherenkov light due to a finite momentum bite is given by:

$$\Delta\theta = \frac{(\Delta p/p)}{\theta}\left(\frac{m^2}{p^2}\right) \tag{4.24}$$

where $\Delta p/p$ is the momentum bite and m is the mass of the particle. From this relation we see that the larger the mass of the particle the larger the broadening. If θ=5 mrad and p=530 GeV, the broadening caused by a 10% momentum bite is

$\Delta\theta_{rms}$ = 1.4 μrad for π's, 17.3 μrad for K's, and 62.6 μrad for p's.

2.7 Beam Divergence

Any divergence in the beam will broaden the angular width of the Cherenkov cone by an equal amount. This is the reason that most Cherenkov counters are located in the parallel sections of the beamlines where the divergence of the beam is deliberately minimized. Typical values for beam divergence in the parallel sections of a beamline are about 0.02–0.10 mrad. The beam divergence in the MW-Beamline varied between 0.025–0.065 mrad depending on the running mode.

4.2.8 Thermal Stability

For Cherenkov counters which employ a gas radiator, one changes the refractive index merely by changing the operating pressure of the counter. The resulting change in the index is given by the Lorentz-Lorenz law:

$$\frac{(\eta^2-1)}{(\eta^2+2)} = \left(\frac{R}{M}\right)\rho \tag{4.25}$$

where R is the molecular refractivity, M is the molecular weight, and ρ is the gas density. For pressures that are not too high (less than 3 atm) Eq. (4.25) can be approximated by:

$$(\eta - 1) = (\eta_0 - 1)P \tag{4.26}$$

where η_0 is the refractive index of the gas for a given wavelength of light, at the temperature of the counter, and at a pressure of 1 atm. The pressure P is in atmospheres. From the last equation we see that the refractive index depends upon the gas density, which depends upon the temperature and pressure according to the equation of state of the gas. Any temperature gradient along the counter can cause variations in the index of refraction and degrade the velocity resolution achievable by the counter. It turns out that:

$$\frac{\Delta\rho}{\rho} = \frac{\Delta P}{P} = -\frac{\Delta T}{T} = \frac{\Delta\beta}{\frac{1}{2}\theta^2} \tag{4.27}$$

where ρ is the gas density, P the pressure and T the temperature. So in order to achieve a resolution of $\Delta\beta = 10^{-7}$ with a Cherenkov angle of 5 mrad we must have a $\Delta T = 2°$C or smaller along the length of the counter.

4.3. The MW Cherenkov Detector

4.3.1 General description

The MW-Cherenkov detector is a gas filled differential counter without an achromatizer. It has however a second larger radius annulus of photodetectors which can be used as an additional particle detection channel or for a veto channel. It is sits in the 67 m long parallel section of the MW-beamline, 708.44 ft (215.93 m) downstream of the MW primary target, and 320.8 ft (97.8m) upstream of the experimental target.

The counter has a total radiator length of 130 ft (42.1 m) and the Cherenkov angle is 4.998 mrad. The counter's pressure vessel consists of two 36 ft. and two 18 ft. stainless steel pipe sections bolted together, plus two 15 ft long aluminum extension pipes at the upstream end to give it a longer radiator length. The inner diameter of the steel pieces is 19.250 in. (48.89cm) and the thickness is 0.375 in. (0.95cm) (Fig. 32).

The counter uses a long (1275.5 in.) focal length mirror to focus the light and two rings at different radii, each with 6 photomultipliers to collect the light. The inner ring of photomultipliers (designated as the coincidence channel) has a radius of 6 3/8 in. (10.19 cm) and the outer ring (anticoincidence or veto channel) has a radius of 7 5/8 in. (19.3 cm).

The counter used He as radiator and the index of refraction was changed by changing the gas pressure. The vessel was checked for leaks and could maintain a

vacuum of 1 mTorr with a rate of rise of 1 mTorr per day. The operating pressure was 4-7 psia and was read remotely by two pressure transducers with an accuracy of ± 0.01 psia. However it was possible to attain 1.2 atm (17 psia) before the pressure relief valve blew. We used two 0.01 in. thick Ti foils for the entrance and exit windows of the counter. Two 4×4 in.^{2} scintillation counters. one upstream and one downstream of the Cherenkov counter, were used in coincidence to define beam particles which passed through the entire counter.

Finally, the vessel of the counter was covered by a 1 in. thick layer of Flex-Sulation X (a foam plastic material) for thermal insulation. The temperature inside the counter was monitored by 6 platinum RTD (resistant transition detectors) that were placed every 18 ft along the counter and measured the temperature with an accuracy of ± 0.2°C.

The MW Cherenkov counter was designed to separate pions from protons at a 530 Gev beam momentum, but the final performance of the counter was such that we were also able to separate pions from kaons. In Table 7 I tabulate the effects the various performance characteristics discussed previously had on the resolution of the MW Cherenkov counter at a 530 GeV mean momentum. We also list the π-K and π-p separation at 530 GeV for comparison.

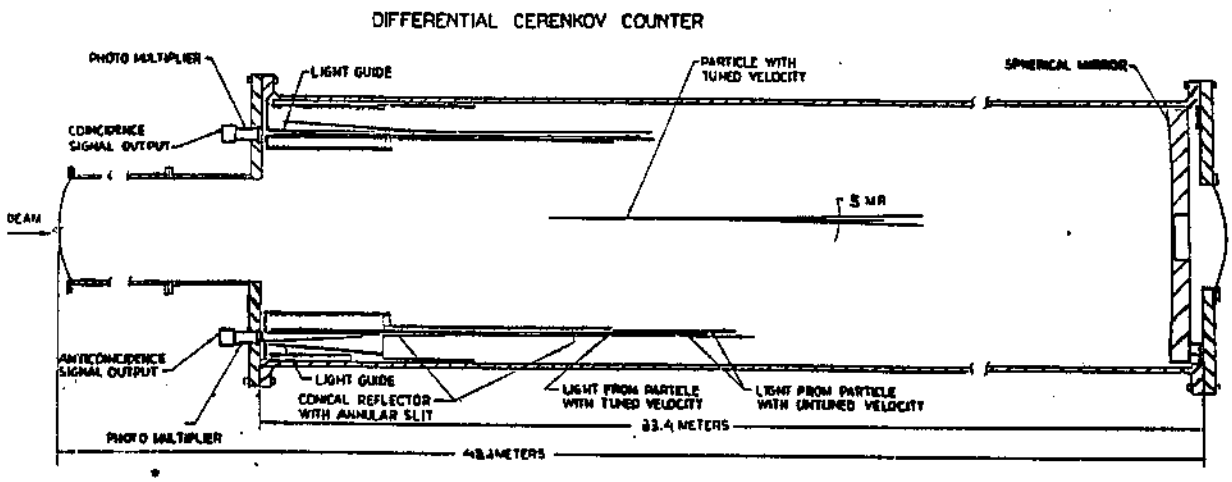

Figure 32: MW Cherenkov counter.

TABLE 7			
Parameter	$\Delta\beta$	$\Delta\theta(mr)$	$\Delta r(mm)$
π p Separation	1.53×10^{-6}	0.306	9.9
π K Separation	4.04×10^{-7}	0.081	2.6
Beam Divergence	1.0×10^{-7}	0.020	0.65
7.0% Momentum Spread	6.10×10^{-8}	0.012	0.40
Temperature to 2°C	7.8×10^{-8}	0.015	0.48
Multiple Scattering	1.5×10^{-8}	0.003	0.09
Chromatic Spread	2.25×10^{-7}	0.045	1.46

TABLE 7: Performance characteristics of the MW-Cherenkov counter at 530 GeV.

4.3.2 The gas system

The gas system for the Cherenkov counter starts at the MW-Gas house in the MW9 enclosure. We used bottles of welding (99.995% pure) He gas. The He bottles were connected at a four station manifold with a Matheson gas regulator and a Scott Speciality moisture trap.

On the upstream end of the counter, and somewhat further downstream, the He gas goes through two more filters before entering the Cherenkov vessel. The first filter was a "shop made" filter consisting of copper brillo pads that were cleaned with freon; this filter is used to prevent oxygen and debris from entering the counter. The second filter is a Scott Specialty gas moisture trap. Before and

after the filters there were pressure gauges to measure any pressure drops.

After the filters, the gas went through a regulator and valve set-up. The valve was used to keep a positive pressure on the regulator. The gas was allowed into the counter by an electric valve. This valve could be operated locally, if the controls were in the "local" mode, or remotely from the experimental counting house, either from a remote control panel or from a personal computer. To prevent overfilling we used a 1.2 atm pressure relief valve located in the middle of the counter.

The Cherenkov counter could be evacuated locally or remotely. The evacuation system used two Guardian "PET 1418" programmable electronic timers that broke the system into three sections. The first opened a solenoid valve, referred to as a "differential pressure module", which allowed the pump and the counter to equalize in pressure, preventing any concussion that could damage the counter's optics when the gate valve was opened.

The second timer opened the gate valve just before the starting of the pump. The gate valve was a VAT VACUUM VALVE, series 10, bought from VAT Inc. in Woburn Mass. It was found that the best setting was for the valve to be fully open about two seconds before the pump started.

The third timer started the pump and the blower at the same time. The pump was an EDWARDS E2M40 with a mechanical booster model EH500A with hydrokinetic drive. The pump had a pumping speed of 400 ft^3 per min at 1 atm.

The pressure of the counter was read from a mechanical pressure gauge and from two pressure transducers. The mechanical pressure gauge was located at the counter and could be read out at the counting house via TV camera and monitor. The pressure transducers were made by OMEGA and were located at the upstream

and downstream end of the counter. Both the transducers were read by a Zenith personal computer using an OMEGA interface card and a terminal box. The gas system is pictured schematically in Fig. 33.

There was also a separate gas system for purging the Cherenkov phototubes with nitrogen, to prevent the phototubes from being contaminated with He (fused silica and natural quartz are permeable to helium). In front of the photomultipliers there were ultrasil (a type of fused silica) windows 3 in. in diameter. The photomultipliers fit in a housing around the windows and sat about 1/2 in. away from them. A gas tight seal was made around the phototubes and the housing to permit a constant nitrogen purge around the phototubes.

The nitrogen gas for the purging comes from a nitrogen dewar outside the experimental building. A line was tapped into the dewar for gas only and the nitrogen was brought to the gas house where there was a check valve and a regulator. After the regulator, the nitrogen was piped to the counter, where it went through a manifold. This manifold distributed the gas to each of the phototubes for purge. A set of 12 oil bubblers on the manifold gave visual evidence that there was a gas purge across the front face of each phototube.

4.3.3 The Optics

The counter optics consisted of a spherical mirror, the conical reflector, the light guides, the phototube windows, and the phototubes.

a) *The spherical mirror.* The mirror that is used to focus the Cherenkov light

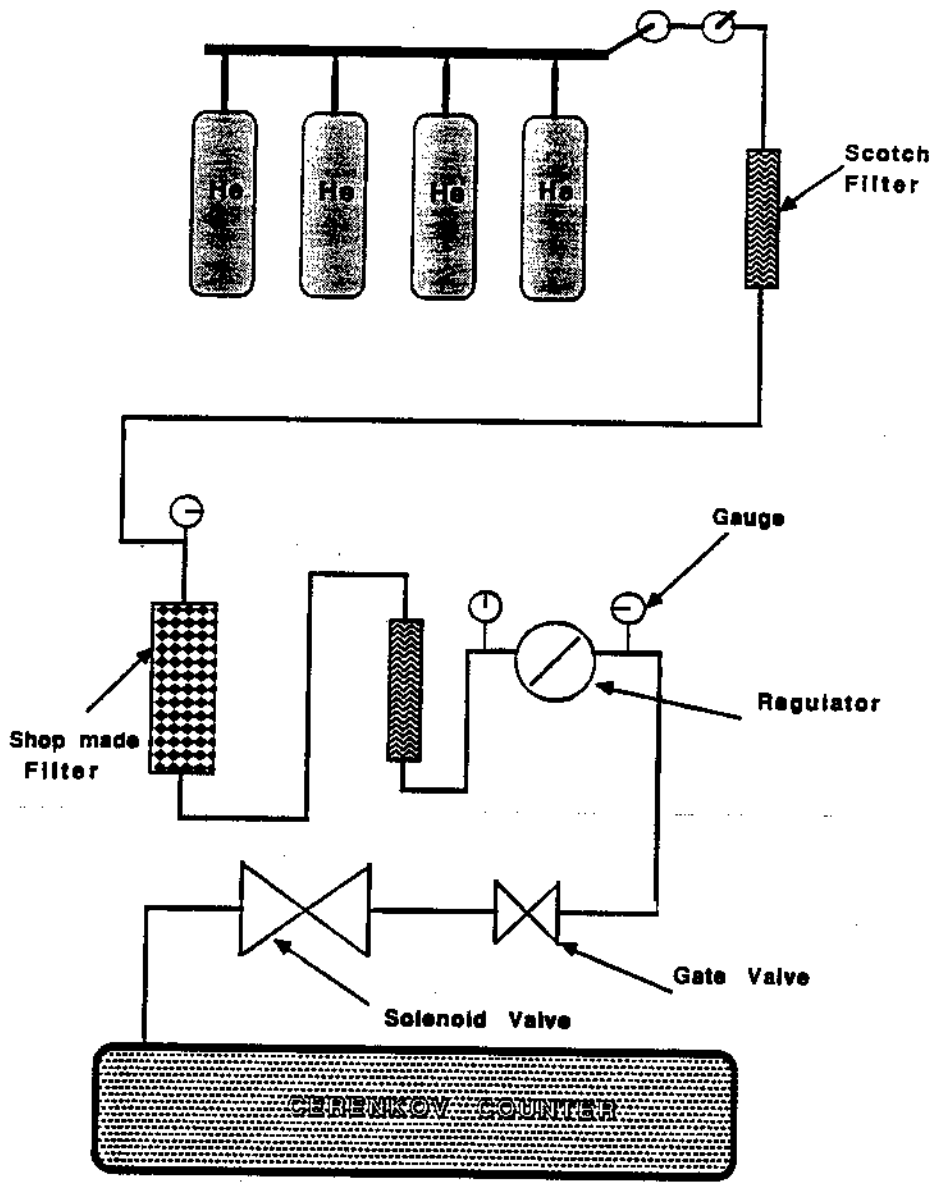

Figure 33: The MW Cherenkov counter gas system

is a front aluminized spherical mirror with a focal length of 1275.5 in. (32.4 m). The mirror (made by Unertl Co. of Philadelphia PA.) has a useful diameter of 18.5 in., and is mounted on a aluminum base that is capable of tilting in the x and y plane for fine adjustments. The mirror was coated with Al plus a $\lambda/2$ thick layer of MgF_2 to protect the Al from oxidizing and enhance the ultraviolet reflectance.

b) *The conical reflector.* The conical reflector consists of a cylinder (45.72 cm long), the front part of which, 16.5 cm, is inclined with a slope of 34.6 mrad. The inner diameter of the cylinder is 29.72 cm (Fig. 34). On top of the cylinder fits a cylindrical cap that has a length of 15.3 cm and a slope of 38.31 mrad. so that there is a gap of 5mm between the cap and the front surface of the cylinder (Fig. 35). Both inclined surfaces are aluminized to reflect the light while the rest surface of the cylinder and the inner surface of the cylindrical cap are painted black to absorb light. In the back of the cylinder fits a ring with openings for the light guides. The counter is tuned by varying the He pressure so that the Cherenkov light of selected or (tagged) particles goes through the 5mm aperture and lands on the inside ring of phototubes (coincidence channel).

The Cherenkov light from particles with masses different from those of the detected particle will hit one of the inclined reflecting surfaces and will end up in the anticoincidence channel of phototubes, or will directly land in the anti-ring of tubes. Of course, if the mass of a particle is much smaller than the mass of the tagged particle, the Cherenkov light of that particle will end up inside the cylinder of the conical reflector and will be lost.

The optical design of the Cherenkov counter was done with the objective of separating πs from ps at the highest possible secondary momentum which was

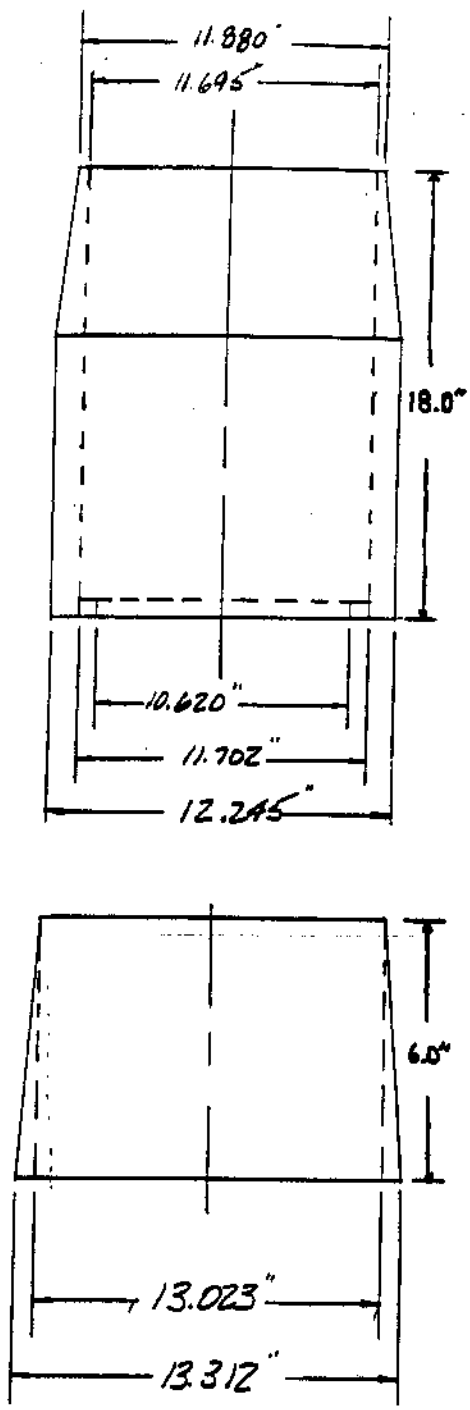

Figure 34: Parts of the Conical Reflector. (top): Main cylinder. (bottom): Cylindrical Cap.

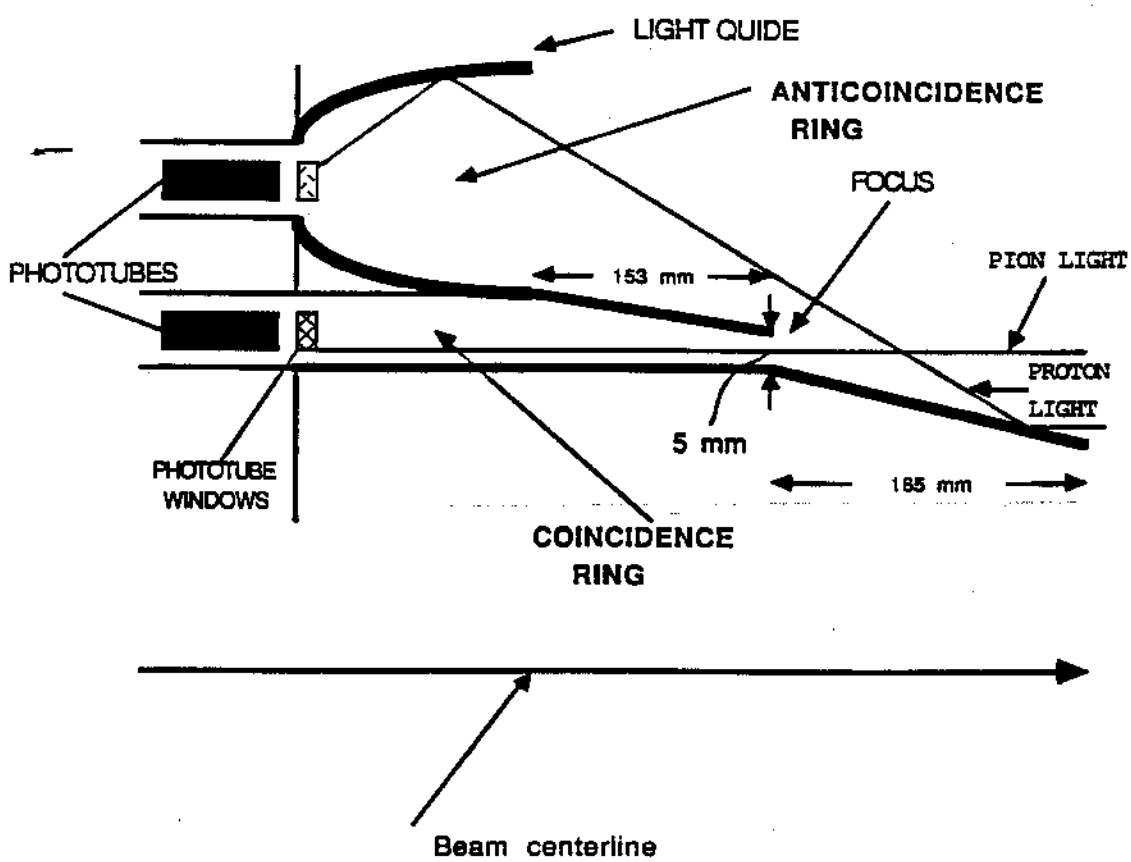

Figure 35: A partial cross section of the conical reflector assembly.

considered to be 700 GeV. For a 700 GeV beam $\Delta\beta_{\pi,p} = 8.778 \times 10^{-7}$ and $\Delta\beta_{\pi,K} = 2.283 \times 10^{-7}$. Thus, for this counter $\Delta\theta_{\pi,p} = \frac{\Delta\beta_{\pi,p}}{tan\theta} = 0.176$ mrad. $\Delta\theta_{\pi,K} = 0.0457$ mrad. Assuming that the tagged particles are pions, the distances, ΔR, between the focal rings are:

$$\Delta R_{\pi,p} = 6.375'' - (1275.5'')\tan(4.822 \text{ mrad}) = 0.224'' = 5.703 \text{ mm} \qquad (4.28)$$

and

$$\Delta R_{\pi,K} = 6.375'' - (1275.5'')\tan(4.953 \text{ mrad}) = 0.057'' = 1.459 \text{ mm} \qquad (4.29)$$

These separations of two particles have to be modified by the effects of divergence of the beam. The beam divergence is, $\Delta\theta_{bd} = \pm 0.025$ mrad. Thus the spread due to the beam divergence is given by:

$$\Delta R_{bd} = \pm f \tan(\theta_{bd}) = \pm 0.0318'' = \pm 0.81 \text{ mm} \qquad (4.30)$$

Now we have to take into account the light spread due to the change in the index of refraction with the wavelength (chromatic spread). The chromatic spread was designed to be confined to the region 0.8 mm from the inner and outer radii of the coincidence ring aperture, to compensate for the smearing due to the beam divergence. In other words the particle's light was restricted to a ring with a width of $(5.0 - 1.6)$ mm=3.4 mm=0.1338 in. centered in the center of the coincidence channel. To restrict the pion or proton light to the desired ring (3.4 mm width), special windows were introduced to block light with wavelengths which corresponded to

undesirable angles. To determine the transmission properties needed for the windows, one wants to position the longest wavelength to which the photocathode is sensitive to (~600 nm), at the smallest Cherenkov angle θ_{min}. Assuming that the tagged particles are pions:

$$\theta^{\pi}_{min} = \frac{\left(6.375'' - \frac{0.1338''}{2}\right)}{1275.5''} = 4.9455 \text{ mrad} \tag{4.31}$$

so:

$$\eta^{\pi}_{min} = \frac{1}{\beta_{\pi} \cos\theta^{\pi}_{min}} = 1.000012250 \tag{4.32}$$

In order to avoid overlapping between pion and proton light, we must have the proton light with the smallest acceptable wavelength lying 0.8 mm away from the 5 mm aperture, i.e:

$$\theta^{p}_{max} = \frac{\left(6.375'' - \frac{0.1968''}{2} - 0.0315''\right)}{1275.5''} = 4.896 \text{ mrad} \tag{4.33}$$

so:

$$\eta^{p}_{max} = \frac{1}{\beta_{p} \cos\theta^{p}_{max}} = 1.000012884 \tag{4.34}$$

We must also confine the pion light with the smallest acceptable wavelength inside the 0.1338" diameter aperture, i.e:

$$\theta^{\pi}_{max} = \frac{\left(6.375'' - \frac{0.1338''}{2}\right)}{1275.5''} = 5.0505 \text{ mrad} \tag{4.35}$$

so:

$$\eta^{\pi}_{max} = \frac{1}{\beta_{\pi} \cos\theta^{\pi}_{max}} = 1.000012775 \tag{4.36}$$

Now taking into account the variation of the index of refraction with the wavelength at 700 GeV (Table 8), we conclude that we must limit the Cherenkov light to be between 220-600 nm. A window can be used to prevent the light below 220 nm from hitting the phototubes. Nothing needs to be done about the light above 600 nm because there are very few photons. For comparison we also list the similar table for 530 GeV (table 9).

From this table we can see that π and p are completely separated at all the wavelengths that the photocathode is sensitive to. In this case the windows reduce the chromatic dispersion of the Cherenkov light and help separate the kaon and pion light. The Cherenkov was used at -530 GeV to tag K^-. In this case we adjusted the Cherenkov pressure so that to position the kaon light with the smallest acceptable wavelength (300 nm as will be explained later) just inside the 0.1338" diameter aperture in the coincidence ring i.e at 6.442" (Table 10). The pion light will end up in the coincidence ring and will overlap with the kaon light for wavelengths larger than 390 nm.

c) *The light guides.* The light guides are used to guide the light through internal reflections to the phototubes. They are made of plastic cold coated internally with

CERENKOV ANGLES WERE CALCULATED AT A MOMENTUM OF 700. GEV/C

WAVELENGTH ANGSTROMS	INDEX AT 5.54 PSI (N-1)*E-5	THETA PIONS IN MR	HEIGHT AT DETECTORS IN IN.	THETA KAONS IN MR	HEIGHT AT DETECTORS IN IN.	THETA PROTONS IN MR	HEIGHT AT DETECTORS IN IN.
1500.	0.1354570	5.2	6.634	5.2	6.577	5.0	6.415
1600.	0.1336058	5.2	6.588	5.1	6.531	5.0	6.368
1700.	0.1321137	5.1	6.552	5.1	6.494	5.0	6.330
1800.	0.1308925	5.1	6.521	5.1	6.463	4.9	6.298
1900.	0.1298789	5.1	6.496	5.0	6.438	4.9	6.272
2000.	0.1290278	5.1	6.474	5.0	6.416	4.9	6.250
2100.	0.1283057	5.1	6.456	5.0	6.398	4.9	6.231
2200.	0.1276873	5.0	6.441	5.0	6.382	4.9	6.215
2300.	0.1271535	5.0	6.427	5.0	6.369	4.9	6.201
2400.	0.1266893	5.0	6.415	5.0	6.357	4.9	6.189
2500.	0.1262829	5.0	6.405	5.0	6.346	4.8	6.178
2600.	0.1259251	5.0	6.396	5.0	6.337	4.8	6.169
2700.	0.1256083	5.0	6.388	5.0	6.329	4.8	6.160
2800.	0.1253265	5.0	6.381	5.0	6.322	4.8	6.153
2900.	0.1250745	5.0	6.374	5.0	6.315	4.8	6.146
3000.	0.1248484	5.0	6.369	4.9	6.310	4.8	6.140
3100.	0.1246446	5.0	6.363	4.9	6.304	4.8	6.135
3200.	0.1244603	5.0	6.359	4.9	6.299	4.8	6.130
3300.	0.1242930	5.0	6.354	4.9	6.295	4.8	6.125
3400.	0.1241409	5.0	6.350	4.9	6.291	4.8	6.121
3500.	0.1240018	5.0	6.347	4.9	6.288	4.8	6.118
3600.	0.1238745	5.0	6.344	4.9	6.284	4.8	6.114
3700.	0.1237577	5.0	6.341	4.9	6.281	4.8	6.111
3800.	0.1236503	5.0	6.338	4.9	6.279	4.8	6.108
3900.	0.1235512	5.0	6.335	4.9	6.276	4.8	6.106
4000.	0.1234596	5.0	6.333	4.9	6.274	4.8	6.103
4100.	0.1233747	5.0	6.331	4.9	6.271	4.8	6.101
4200.	0.1232960	5.0	6.329	4.9	6.269	4.8	6.099
4300.	0.1232228	5.0	6.327	4.9	6.267	4.8	6.097
4400.	0.1231546	5.0	6.325	4.9	6.266	4.8	6.095
4500.	0.1230910	5.0	6.323	4.9	6.264	4.8	6.093
4600.	0.1230318	5.0	6.322	4.9	6.262	4.8	6.092
4700.	0.1229760	5.0	6.321	4.9	6.261	4.8	6.090
4800.	0.1229239	5.0	6.319	4.9	6.260	4.8	6.089
4900.	0.1228750	5.0	6.318	4.9	6.258	4.8	6.088
5000.	0.1228290	5.0	6.317	4.9	6.257	4.8	6.086
5100.	0.1227858	5.0	6.316	4.9	6.256	4.8	6.085
5200.	0.1227450	5.0	6.315	4.9	6.255	4.8	6.084
5300.	0.1227066	4.9	6.314	4.9	6.254	4.8	6.083
5400.	0.1226703	4.9	6.313	4.9	6.253	4.8	6.082
5500.	0.1226360	4.9	6.312	4.9	6.252	4.8	6.081
5600.	0.1226035	4.9	6.311	4.9	6.251	4.8	6.080
5700.	0.1225728	4.9	6.310	4.9	6.251	4.8	6.080
5800.	0.1225436	4.9	6.309	4.9	6.250	4.8	6.079
5900.	0.1225160	4.9	6.309	4.9	6.249	4.8	6.078
6000.	0.1224897	4.9	6.308	4.9	6.248	4.8	6.077

Table 8: Variation of the index of refraction of He and the Cherenkov angle of different 700 GeV particles with the wavelength. The index of refraction of He was calculated at a pressure of 5.54 psi and at 20°. *(Height at the detectors means radius at the phototubes).

CERENKOV ANGLES WERE CALCULATED AT A MOMENTUM OF 530. GEV/C

WAVELENGTH ANGSTROMS	INDEX AT 5.55 PSI (N-1)*E-5	THETA PIONS IN MR	HEIGHT AT DETECTORS IN IN.	THETA KAONS IN MR	HEIGHT AT DETECTORS IN IN.	THETA PROTONS IN MR	HEIGHT AT DETECTORS IN IN.
1500.	0.1356216	5.2	6.634	5.1	6.535	4.9	6.248
1600.	0.1337679	5.2	6.589	5.1	6.489	4.9	6.199
1700.	0.1322743	5.1	6.552	5.1	6.451	4.8	6.160
1800.	0.1310516	5.1	6.521	5.0	6.420	4.8	6.127
1900.	0.1300368	5.1	6.496	5.0	6.395	4.8	6.100
2000.	0.1291846	5.1	6.475	5.0	6.373	4.8	6.078
2100.	0.1284616	5.1	6.456	5.0	6.355	4.7	6.058
2200.	0.1278425	5.0	6.441	5.0	6.339	4.7	6.042
2300.	0.1273080	5.0	6.427	5.0	6.325	4.7	6.027
2400.	0.1268432	5.0	6.416	4.9	6.313	4.7	6.015
2500.	0.1264364	5.0	6.405	4.9	6.302	4.7	6.004
2600.	0.1260782	5.0	6.396	4.9	6.293	4.7	5.994
2700.	0.1257610	5.0	6.388	4.9	6.285	4.7	5.985
2800.	0.1254788	5.0	6.381	4.9	6.278	4.7	5.978
2900.	0.1252265	5.0	6.374	4.9	6.271	4.7	5.971
3000.	0.1250001	5.0	6.369	4.9	6.265	4.7	5.965
3100.	0.1247961	5.0	6.363	4.9	6.260	4.7	5.959
3200.	0.1246116	5.0	6.359	4.9	6.255	4.7	5.954
3300.	0.1244441	5.0	6.354	4.9	6.251	4.7	5.949
3400.	0.1242917	5.0	6.350	4.9	6.247	4.7	5.945
3500.	0.1241525	5.0	6.347	4.9	6.243	4.7	5.941
3600.	0.1240251	5.0	6.344	4.9	6.240	4.7	5.938
3700.	0.1239082	5.0	6.341	4.9	6.237	4.7	5.935
3800.	0.1238006	5.0	6.338	4.9	6.234	4.7	5.932
3900.	0.1237013	5.0	6.335	4.9	6.231	4.6	5.929
4000.	0.1236096	5.0	6.333	4.9	6.229	4.6	5.927
4100.	0.1235247	5.0	6.331	4.9	6.227	4.6	5.924
4200.	0.1234458	5.0	6.329	4.9	6.225	4.6	5.922
4300.	0.1233726	5.0	6.327	4.9	6.223	4.6	5.920
4400.	0.1233043	5.0	6.325	4.9	6.221	4.6	5.918
4500.	0.1232406	5.0	6.324	4.9	6.219	4.6	5.916
4600.	0.1231811	5.0	6.322	4.9	6.218	4.6	5.915
4700.	0.1231255	5.0	6.321	4.9	6.216	4.6	5.913
4800.	0.1230733	5.0	6.319	4.9	6.215	4.6	5.912
4900.	0.1230243	5.0	6.318	4.9	6.214	4.6	5.910
5000.	0.1229783	5.0	6.317	4.9	6.213	4.6	5.909
5100.	0.1229350	5.0	6.316	4.9	6.211	4.6	5.908
5200.	0.1228942	5.0	6.315	4.9	6.210	4.6	5.907
5300.	0.1228557	4.9	6.314	4.9	6.209	4.6	5.906
5400.	0.1228194	4.9	6.313	4.9	6.208	4.6	5.905
5500.	0.1227851	4.9	6.312	4.9	6.207	4.6	5.904
5600.	0.1227526	4.9	6.311	4.9	6.207	4.6	5.903
5700.	0.1227218	4.9	6.310	4.9	6.206	4.6	5.902
5800.	0.1226926	4.9	6.309	4.9	6.205	4.6	5.901
5900.	0.1226649	4.9	6.309	4.9	6.204	4.6	5.901
6000.	0.1226386	4.9	6.308	4.9	6.204	4.6	5.900

Table 9: Variation of the index of refraction of He and the Cherenkov angle of different 530 GeV particles with the wavelength. The index of refraction of He was calculated at a pressure of 5.55 psi and at 20°.

CERENKOV ANGLES WERE CALCULATED AT A MOMENTUM OF 530. GEV/C

WAVELENGTH ANGSTROMS	INDEX AT 5.86 PSI (N-1)*E-5	THETA PIONS IN MR	HEIGHT AT DETECTORS IN IN.	THETA KAONS IN MR	HEIGHT AT DETECTORS IN IN.	THETA PROTONS IN MR	HEIGHT AT DETECTORS IN IN.
1500.	0.1431098	5.3	6.816	5.3	6.719	5.0	6.440
1600.	0.1411538	5.3	6.769	5.2	6.672	5.0	6.390
1700.	0.1395777	5.3	6.731	5.2	6.633	5.0	6.350
1800.	0.1382874	5.3	6.699	5.2	6.601	5.0	6.317
1900.	0.1372166	5.2	6.673	5.2	6.575	4.9	6.289
2000.	0.1363174	5.2	6.651	5.1	6.553	4.9	6.266
2100.	0.1355545	5.2	6.633	5.1	6.534	4.9	6.246
2200.	0.1349012	5.2	6.617	5.1	6.517	4.9	6.229
2300.	0.1343372	5.2	6.603	5.1	6.503	4.9	6.214
2400.	0.1338468	5.2	6.591	5.1	6.491	4.9	6.201
2500.	0.1334175	5.2	6.580	5.1	6.480	4.9	6.190
2600.	0.1330395	5.2	6.571	5.1	6.471	4.8	6.180
2700.	0.1327048	5.1	6.562	5.1	6.462	4.8	6.171
2800.	0.1324070	5.1	6.555	5.1	6.455	4.8	6.163
2900.	0.1321408	5.1	6.548	5.1	6.448	4.8	6.156
3000.	0.1319019	5.1	6.543	5.1	6.442	4.8	6.150
3100.	0.1316866	5.1	6.537	5.0	6.437	4.8	6.144
3200.	0.1314919	5.1	6.532	5.0	6.432	4.8	6.139
3300.	0.1313152	5.1	6.528	5.0	6.427	4.8	6.134
3400.	0.1311543	5.1	6.524	5.0	6.423	4.8	6.130
3500.	0.1310075	5.1	6.520	5.0	6.419	4.8	6.126
3600.	0.1308730	5.1	6.517	5.0	6.416	4.8	6.123
3700.	0.1307496	5.1	6.514	5.0	6.413	4.8	6.119
3800.	0.1306361	5.1	6.511	5.0	6.410	4.8	6.116
3900.	0.1305314	5.1	6.508	5.0	6.407	4.8	6.114
4000.	0.1304346	5.1	6.506	5.0	6.405	4.8	6.111
4100.	0.1303450	5.1	6.504	5.0	6.403	4.8	6.109
4200.	0.1302618	5.1	6.502	5.0	6.400	4.8	6.106
4300.	0.1301844	5.1	6.500	5.0	6.398	4.8	6.104
4400.	0.1301124	5.1	6.498	5.0	6.397	4.8	6.102
4500.	0.1300452	5.1	6.496	5.0	6.395	4.8	6.101
4600.	0.1299825	5.1	6.495	5.0	6.393	4.8	6.099
4700.	0.1299237	5.1	6.493	5.0	6.392	4.8	6.097
4800.	0.1298687	5.1	6.492	5.0	6.390	4.8	6.096
4900.	0.1298170	5.1	6.491	5.0	6.389	4.8	6.095
5000.	0.1297684	5.1	6.489	5.0	6.388	4.8	6.093
5100.	0.1297227	5.1	6.488	5.0	6.387	4.8	6.092
5200.	0.1296797	5.1	6.487	5.0	6.386	4.8	6.091
5300.	0.1296391	5.1	6.486	5.0	6.385	4.8	6.090
5400.	0.1296008	5.1	6.485	5.0	6.384	4.8	6.089
5500.	0.1295645	5.1	6.484	5.0	6.383	4.8	6.088
5600.	0.1295302	5.1	6.483	5.0	6.382	4.8	6.087
5700.	0.1294977	5.1	6.482	5.0	6.381	4.8	6.086
5800.	0.1294669	5.1	6.482	5.0	6.380	4.8	6.085
5900.	0.1294377	5.1	6.481	5.0	6.379	4.8	6.084
6000.	0.1294099	5.1	6.480	5.0	6.379	4.8	6.084

Table 10: Variation of the index of refraction of He and the Cherenkov angle of different 530 GeV particles with the wavelength. The index of refraction of He was calculated at a pressure of 5.86 psi and at 20°.

Al and they have a conical shape with a round top.

d) *The phototube windows.* The windows in front of the phototubes have a diameter of 3 in. (7.62 cm) and the ones in front of the inner (coincidence) ring of phototubes have a thickness of 1/2 in. (1.27 cm) while the ones in front of the outer (anti-coincidence) ring of phototubes have a thickness of 3/4 in. (1.91 cm). All the windows in the coincidence channel are made of Ultrasil and they effectively transmit light down to 225 nm (Fig. 36). In the anticoincidence or outer ring, the windows were made of an unknown type of UV glass whose transmission dropped severely below 300 nm.

e) *The phototubes.* HAMAMATSU R1332X phototubes with quartz windows were used, which are capable of detecting light down to 160 nm. The phototubes have a 2 in. (51 mm) diameter and use a bialkali photocathode for high quantum efficiency (25% at 385 nm). The quantum efficiency of the phototubes is plotted versus wavelength in Fig. 37.

4.3.4 Logic and Electronics

The signals from all the phototubes and the two scintillation counters upstream and downstream the Cherenkov counter are transported using coaxial cables to the upstream latch house where they go through the electronics.

The Cherenkov trigger logic is depicted schematically in Fig. 38. The phototube signals are first amplified by a programmable amplifier, set to a gain of ten, and then go through a discriminator (along with the signals of the two scintillators).

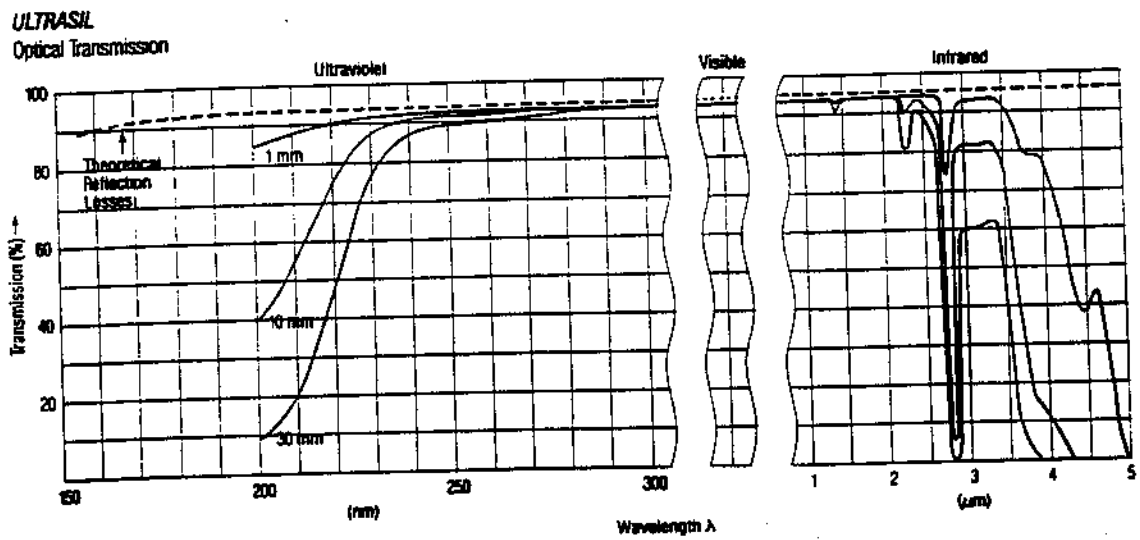

Figure 36: Optical transmission of the Ultrasil windows.

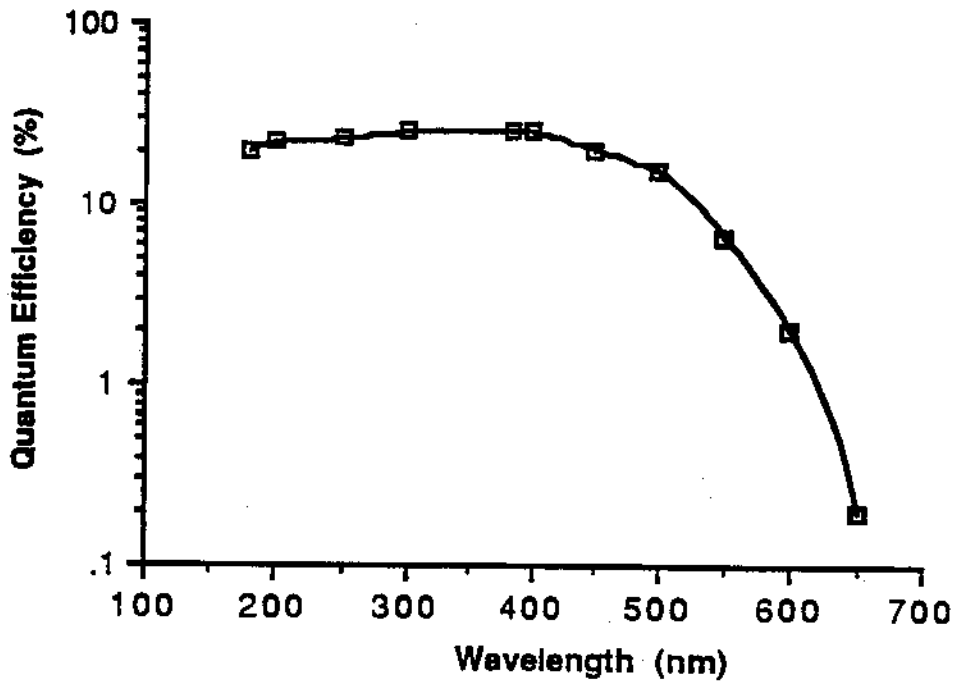

Figure 37: Quantum efficiency versus wavelength, for the HAMAMATSU R1332X phototubes.

After the discriminator, the signals go to a programmable logic delay/fan-out unit for timing. This unit has three output streams.

The first stream of output signals goes to a series of 4508 LeCroy programmable logic units used to do the final Cherenkov coincidence logic. The 6 Cherenkov coincidence logic combinations outputs along with the two signals from the scintillation counters, go through an ECL/NIM converter, then to a prescaler and finally to a scaler from where they are recorded. These signals were used to obtain the Cherenkov pressure curves. The Cherenkov coincidence logic combinations used were:

$DN_1\overline{VN_2}$: N_1 or more phototubes in the coincidence channel firing with less than N_2 phototubes firing in the anti-coincidence channel ($1 \leq N_{1,2} \leq 6$). In this notation D stands for the coincidence channel and V for the anti-coincidence (veto channel).

$D23\overline{V2}$: $[(1.AND.3.AND.5).OR.(2.AND.4.AND.6)]$ .AND.$\overline{V2}$ where the numbers correspond to photomultipliers in the coincidence channel if one starts counting them from the top and goes clockwise looking downstream along the direction of the beam.

A second and the third streams of signals go to latches designed by our University of Minnesota collaborators. For each event the content of the Cherenkov latches were written to a tape along with the other event information. Out of the 16 data bits avaliable in the Cherenkov latches, 6 were used to store the information from the phototubes in the coincidence channel, 6 to store the information from the phototubes in the anti-channel and 2 to store the information from the two Cherenkov scintillators counters.

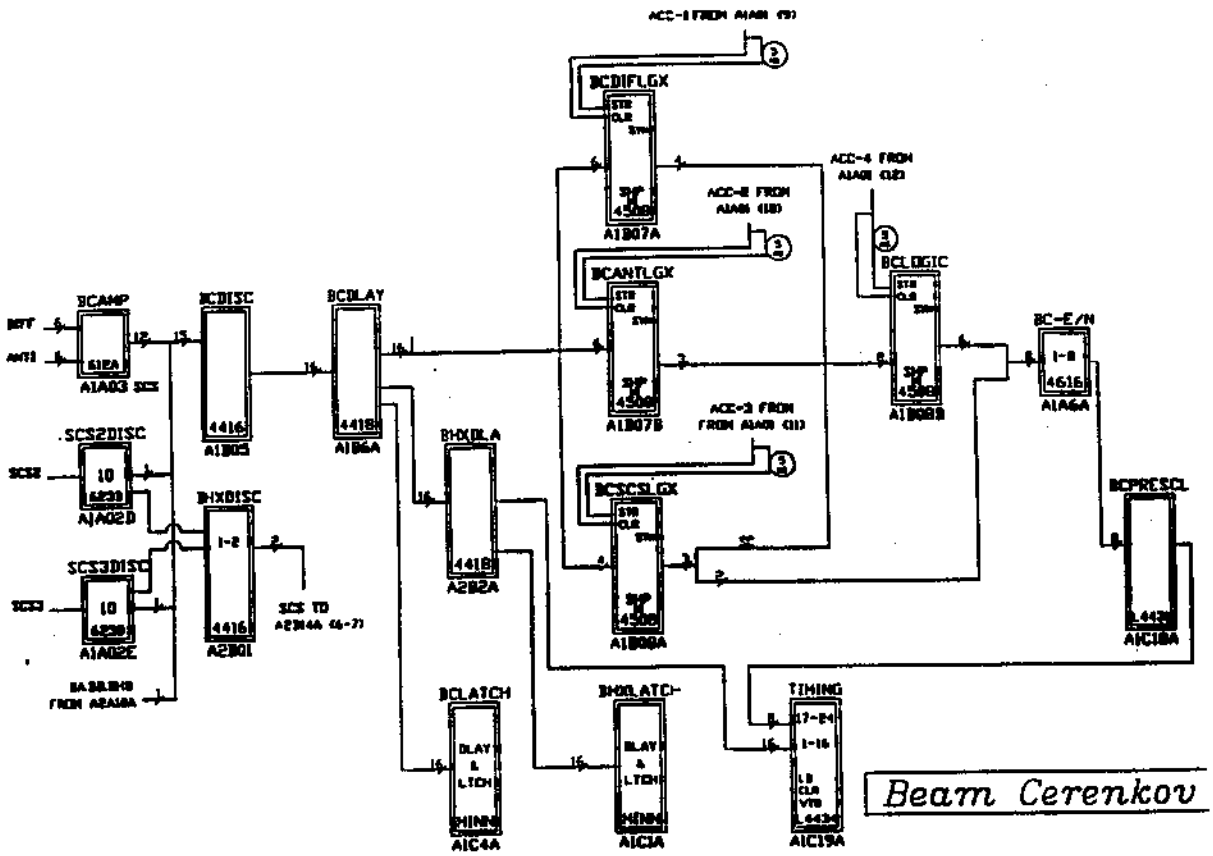

Figure 38: MW Cherenkov trigger logic.

All the high voltage signals were controlled by a Le Croy 1440 programmable multichannel high voltage supply.

4.4. Monte Carlo Simulation and Counter Performance

4.4.1 Monte Carlo Simulation and Pressure Curves

The MW-Cherenkov counter was used extensively during the E-706 shakedown run to tag particles at different momenta in the range 50-530 GeV and at + and − polarities. In Fig. 39, 40, 41 and 42 a set of pressure curves taken at several different momenta and polarities are shown. As we can see from the pressure curves, there is a separation (although not complete) between π and K even at 530 GeV.

A Monte Carlo program was developed to simulate the counter's performance in order to help us estimate the exact kaon and pion fraction at 530 GeV, and the various contaminations. The Monte Carlo program generates particles of specified masses taking into account the momentum dispersion of the beam. Each particle emits Cherenkov radiation at random points along its path through the counter. The photons are generated uniformly within a wavelength range accepted by the counter's optics. For each wavelength the refractive index of He was calculated using the Dalgano and Kingston expression (Eq. 4.17), and then was converted to

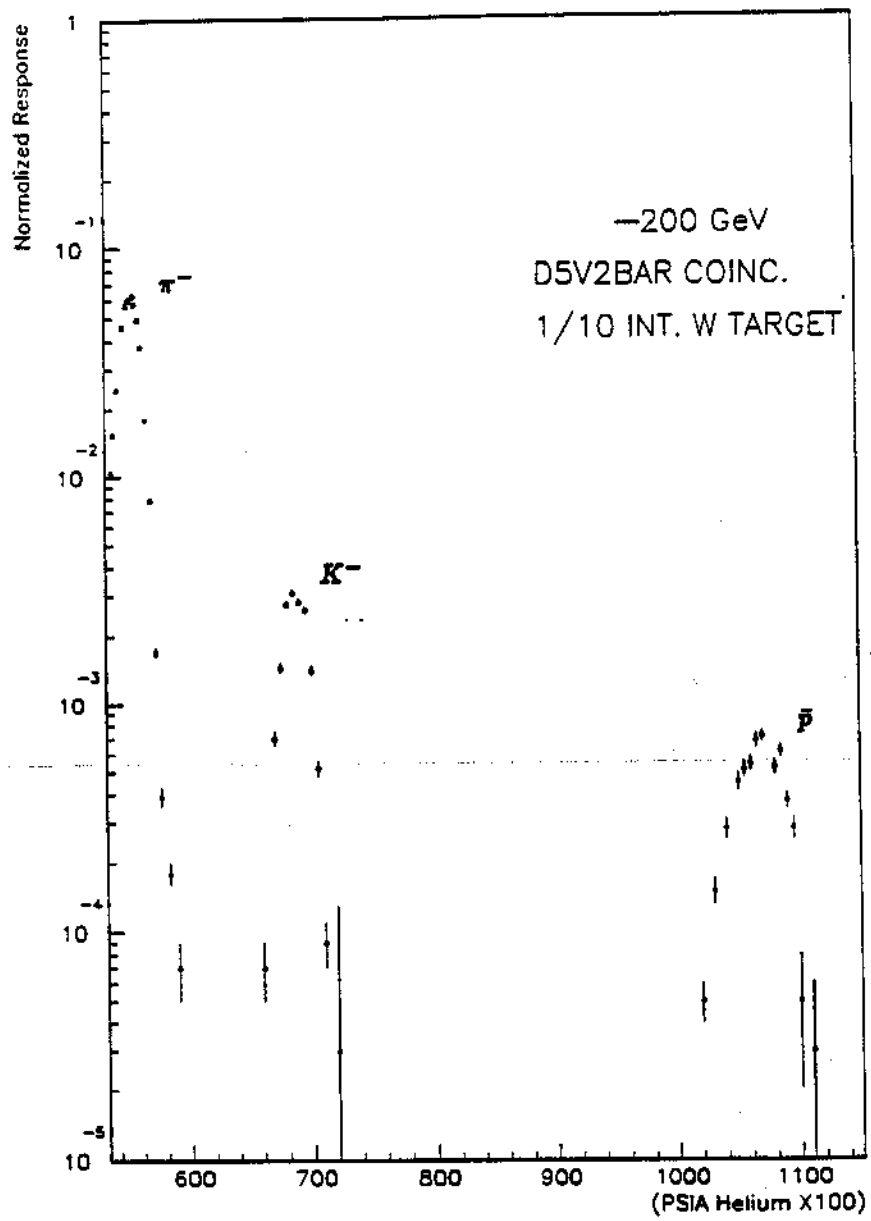

Figure 39: Pressure Curve at -200 GeV.

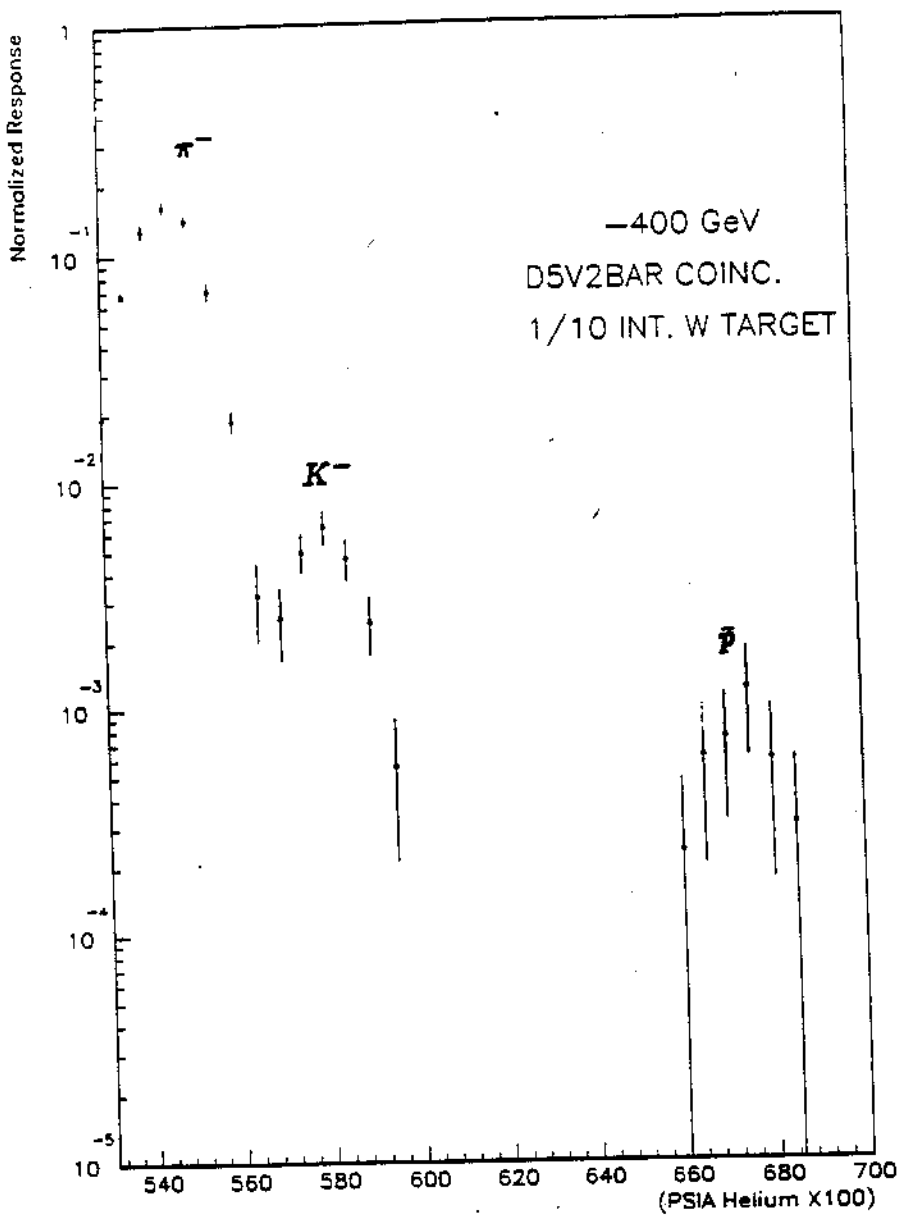

Figure 40: Pressure Curve at -400 GeV.

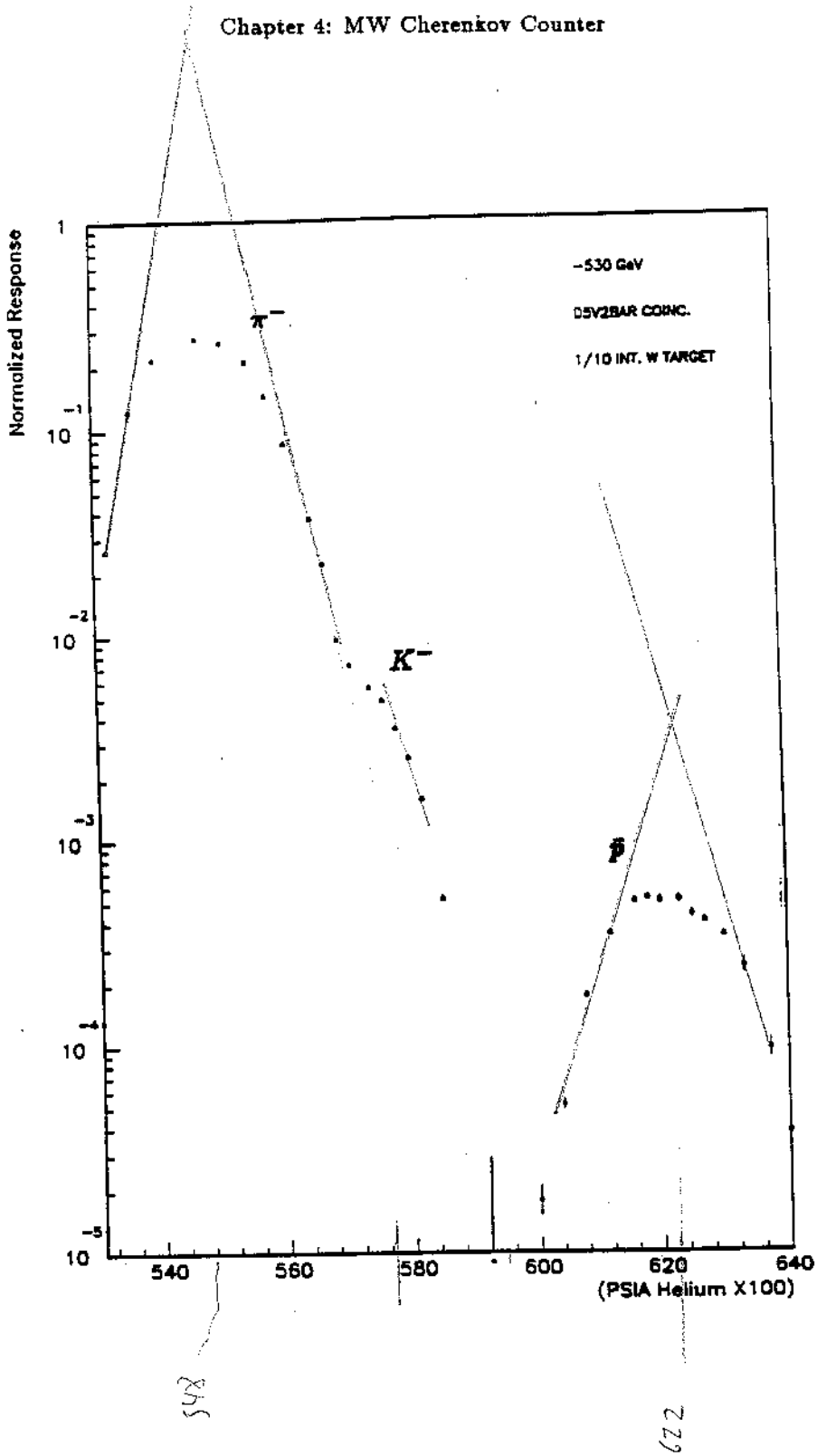

Figure 41: Pressure Curve at -530 GeV.

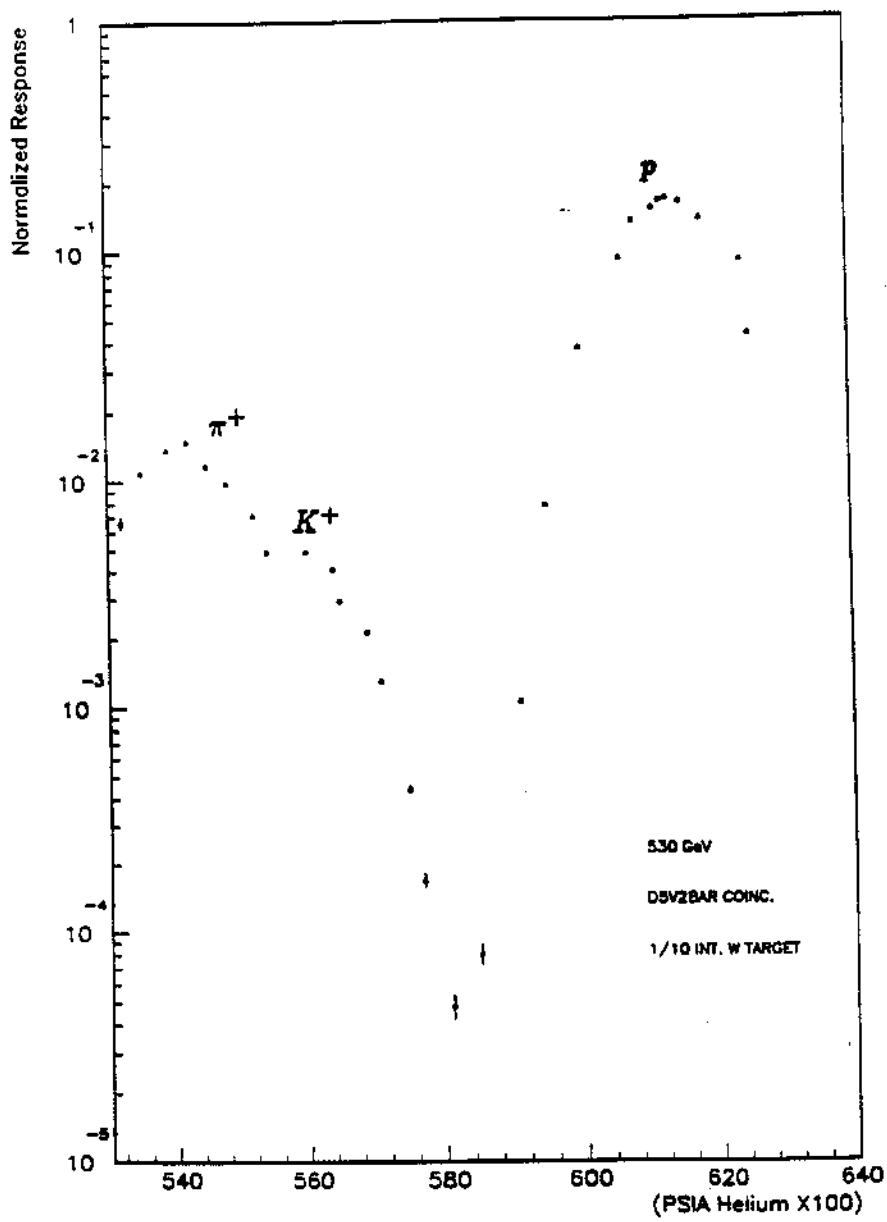

Figure 42: Pressure Curve at 530 GeV.

the pressure and temperature of the counter using the Lorentz-Lorenz law and the law of gases. The emission of photons was considered to take place at a cone polar angle $\theta = \cos^{-1}(1/\eta\beta)$ and to be uniform in ϕ. Finally each photon was weighted with the probability $dN/d\lambda = (2\pi\alpha/\lambda^2)L\sin^2\theta$, where $dN/d\lambda$ is the number of photons per wavelength, L is the counter's length, and α is the fine structure constant. The beam divergence of the beam was added as Gaussian distribution in the angle θ.

The emitted photons are reflected from the mirror and are followed through the counter. The ones that make it to the phototubes are transformed into photoelectrons using the quantum efficiency curves. Using the number of photoelectrons the various electronic efficiencies are calculated and plotted as a function of pressure.

The Monte Carlo pressure curves were also used to qualitatively show the effect of the chromatic dispersion, the beam divergence and the beam momentum bite on the counter's resolution. Figures 43, 44 and 45 show the effect that each of the quantities mentioned above had on the Cherenkov pressure curve at -530 GeV. The particles fractions used in these examples were determined from the data. Figures 46, 47 show the Monte Carlo pressure curves superimposed on the actual pressure curves for the ± 530 GeV and the $D5\overline{V2}$ coincidence level (for the 3/4 interaction length Al target). The agreement between the calculations and the data is good.

Although the optical properties of the mirror, the phototube windows and the phototubes are well known, there was some uncertainty concerning the optical properties of the various light guides. After studying the efficiencies for the six-fold coincidence ($D6$) achieved by the counter ($\sim 8.0\%$), we concluded that we

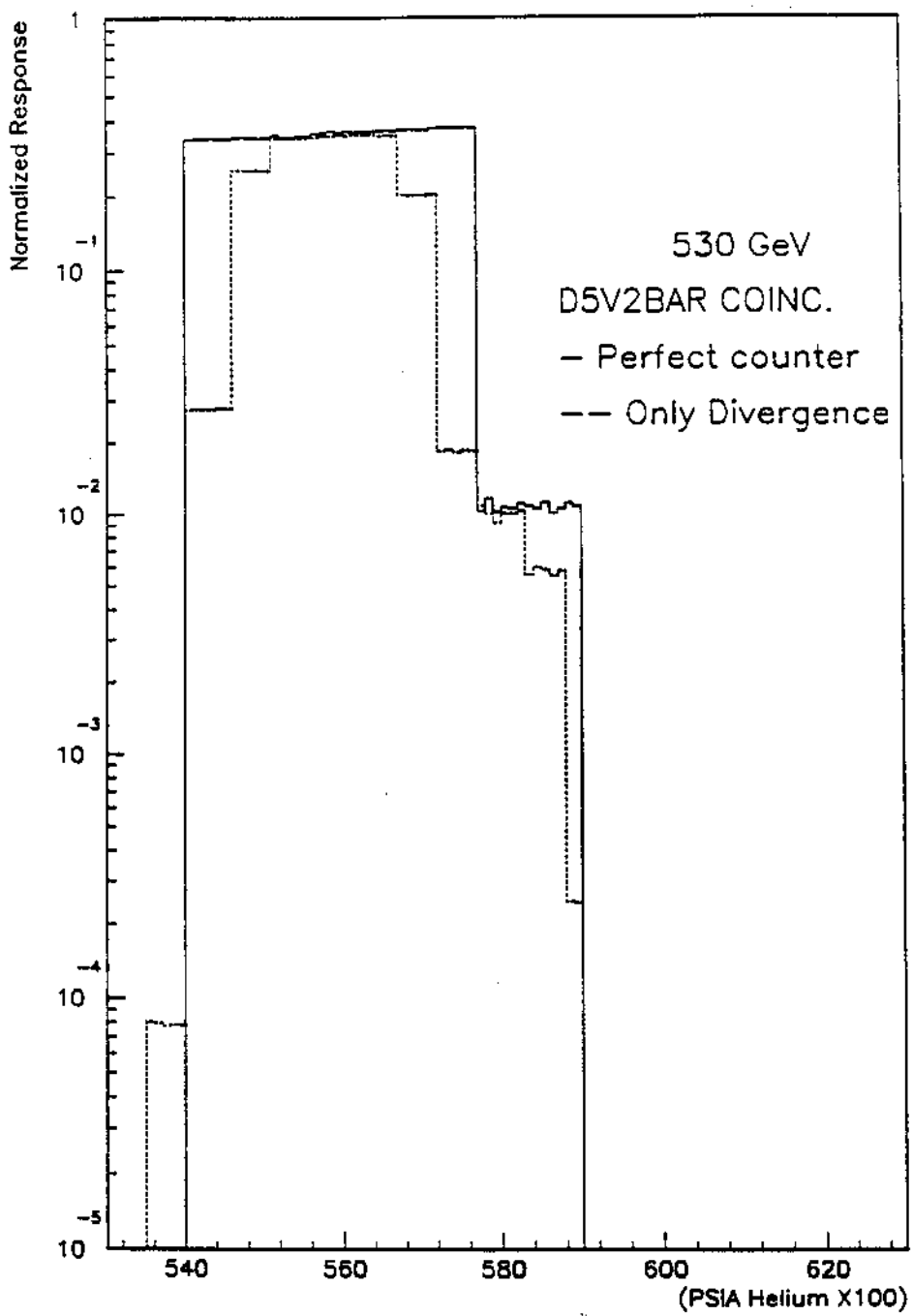

Figure 43: Effect of the beam divergence on the resolution of the Cherenkov counter at -530 GeV. Solid line: Perfect counter. Dashed line: Counter with only beam divergence (0.025 mrad).

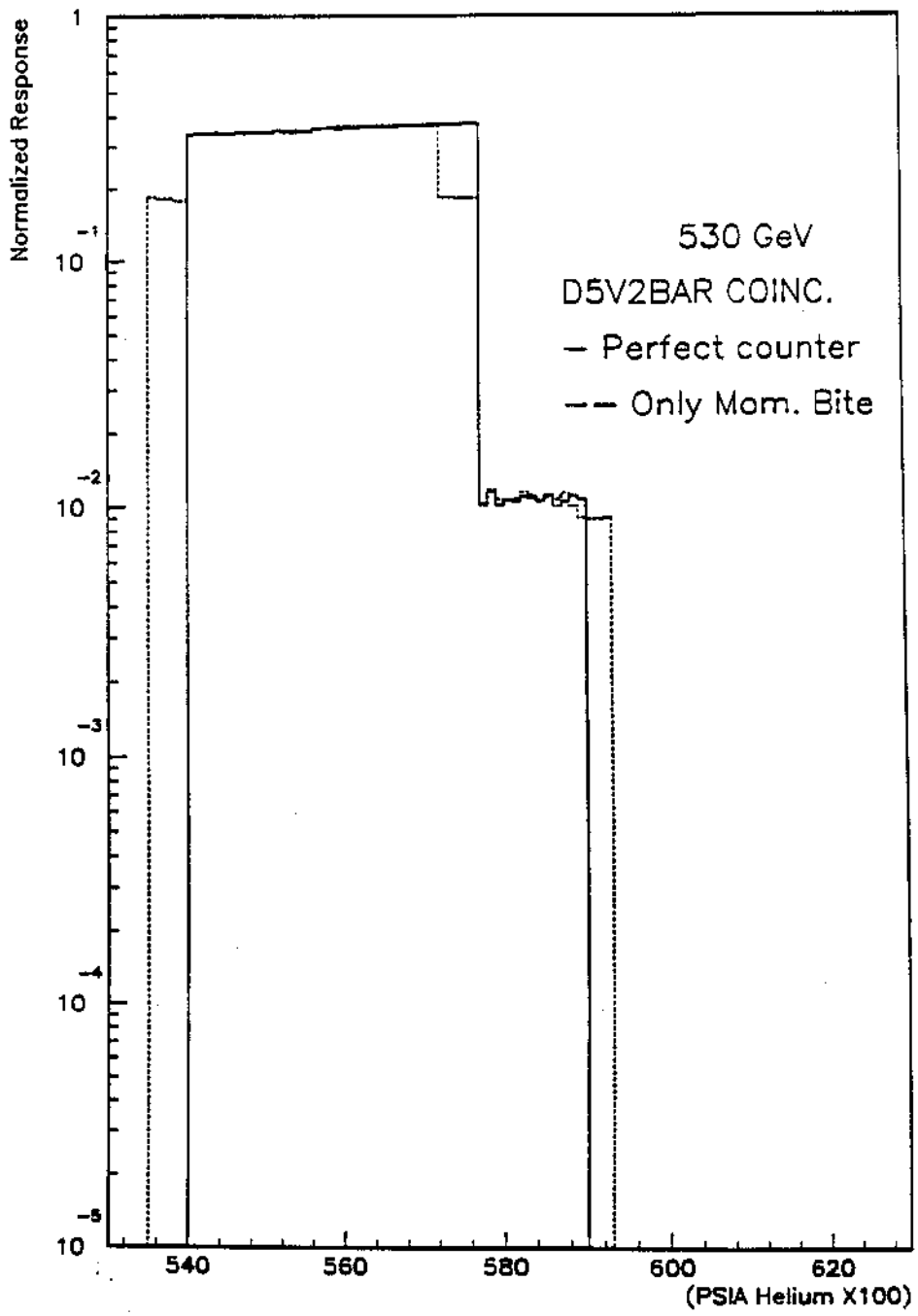

Figure 44: Effect of the beam momentum bite on the resolution of the Cherenkov counter. Solid line: Perfect counter Dashed line: Counter with 10% (FWHM) momentum bite.

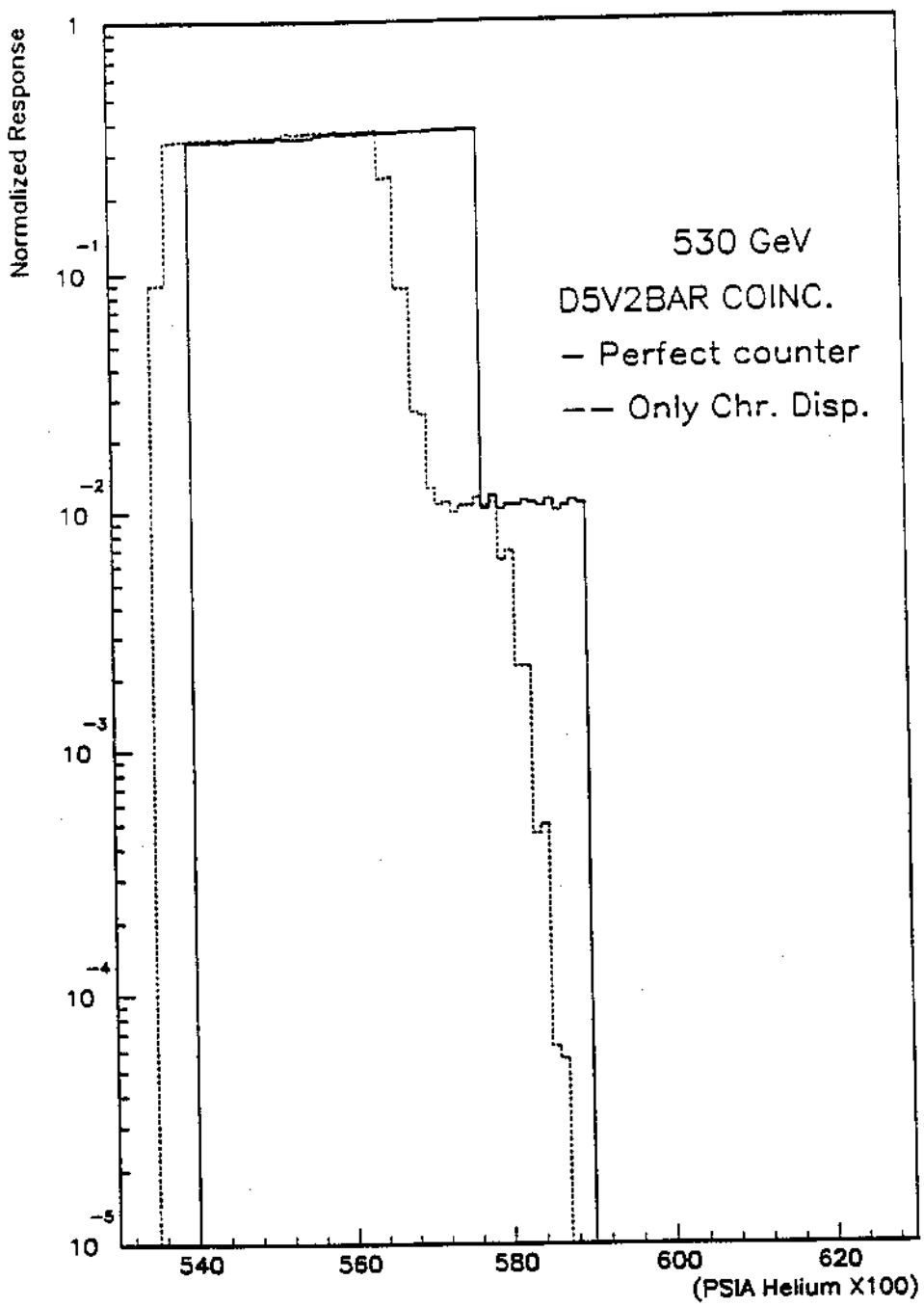

Figure 45: Effect of the chromatic dispersion to the resolution of the Cherenkov counter. Solid line: Perfect counter. Dashed line: Counter with only chromatic dispersion.

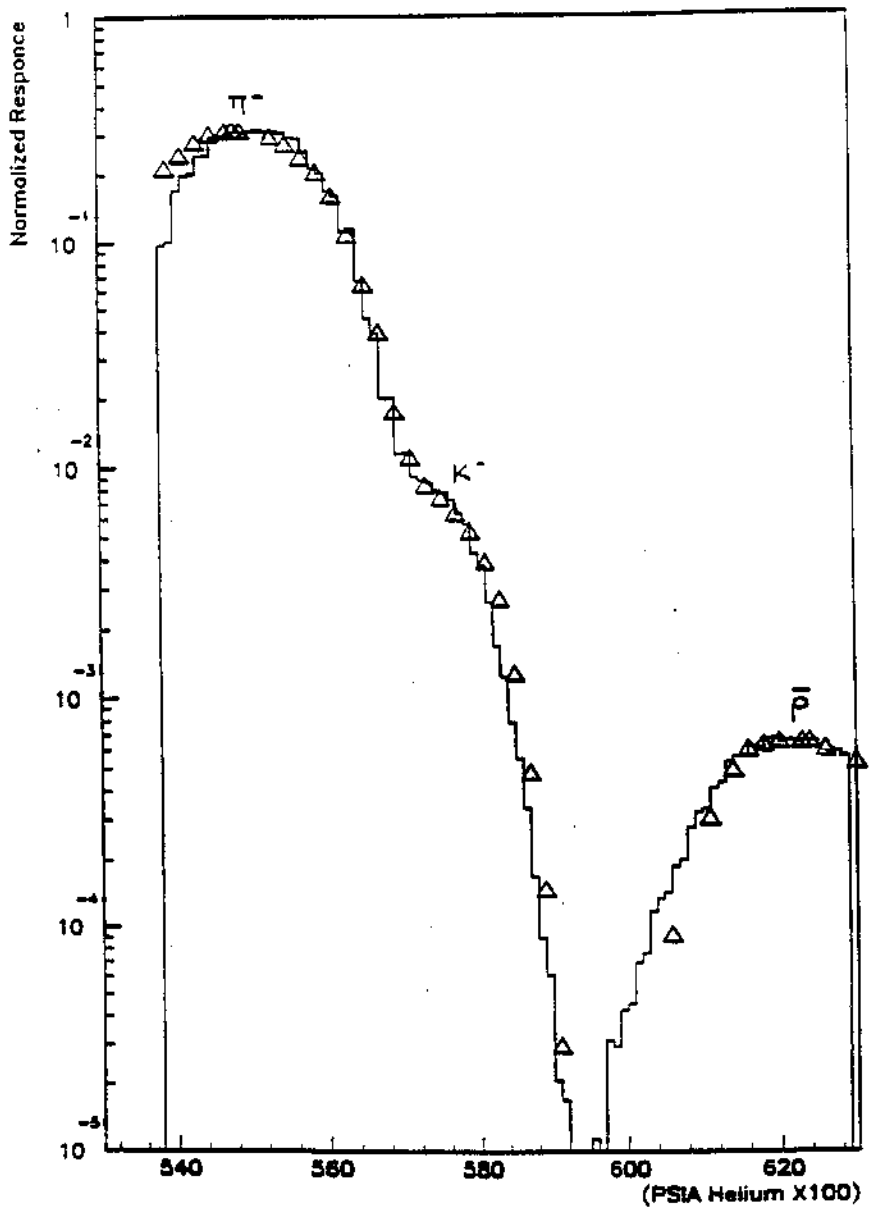

Figure 46: Comparison of the Monte Carlo pressure curve to the experimental data one at -530 GeV for the 3/4 interaction length Al target and the $D5\overline{V2}$ coincidence level.

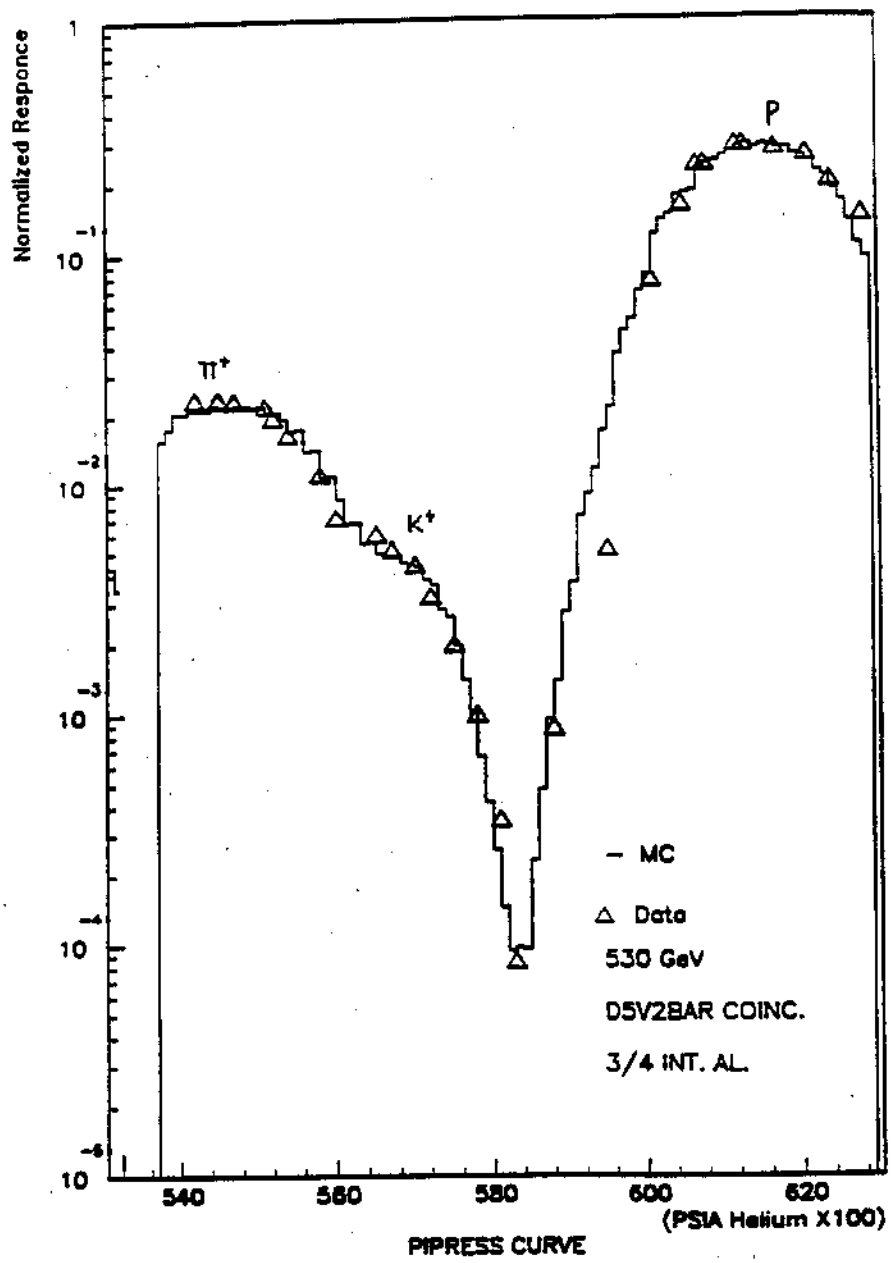

Figure 47: Comparison of the Monte Carlo pressure curve to the experimental data one at 530 GeV for the 3/4 interaction length Al target and the $D5\overline{V2}$ coincidence level.

were getting 1.1 photoelectrons per phototube per particle which is about half of what was expected, if the counter's optics were reflecting down to 220 nm as expected. This suggests the fact that most of the short wavelength photons were absorbed by the plastic light guides. This loss of light was responsible for the low observed efficiencies but also had a beneficial effect which was an improvement in the counter's resolution because the chromatic dispersion decreased. As a result the π-K resolution improved. This observation was also confirmed by the Monte Carlo program (Fig. 48). The best estimate of the actual accepted wavelength range is 300-600 nm.

4.4.2 Negative Beam Tagging

The negative 530 GeV beam that was used during the last E-706 run was composed mostly of π^- ($\sim 97\%$) and K^- ($\sim 3\%$). The fraction of antiprotons was small$\sim 0.2\%$. The Cherenkov counter was used to tag the minority particles (K^-), and everything that was not tagged as a K^- was called a π^- (the antiprotons were ignored).

The coincidence requirement that was chosen for tagging was $D4\overline{V2}$ which was the most efficient with sufficient separation between πs and Ks. The pressure point at which the counter was set was chosen so as to tag as many K^-s as possible, with the smallest possible contamination.

The exact composition of the negative beam at 530 GeV was determined by fitting the M.C pressure curve to the experimental one for the $D5\overline{V2}$ coincidence

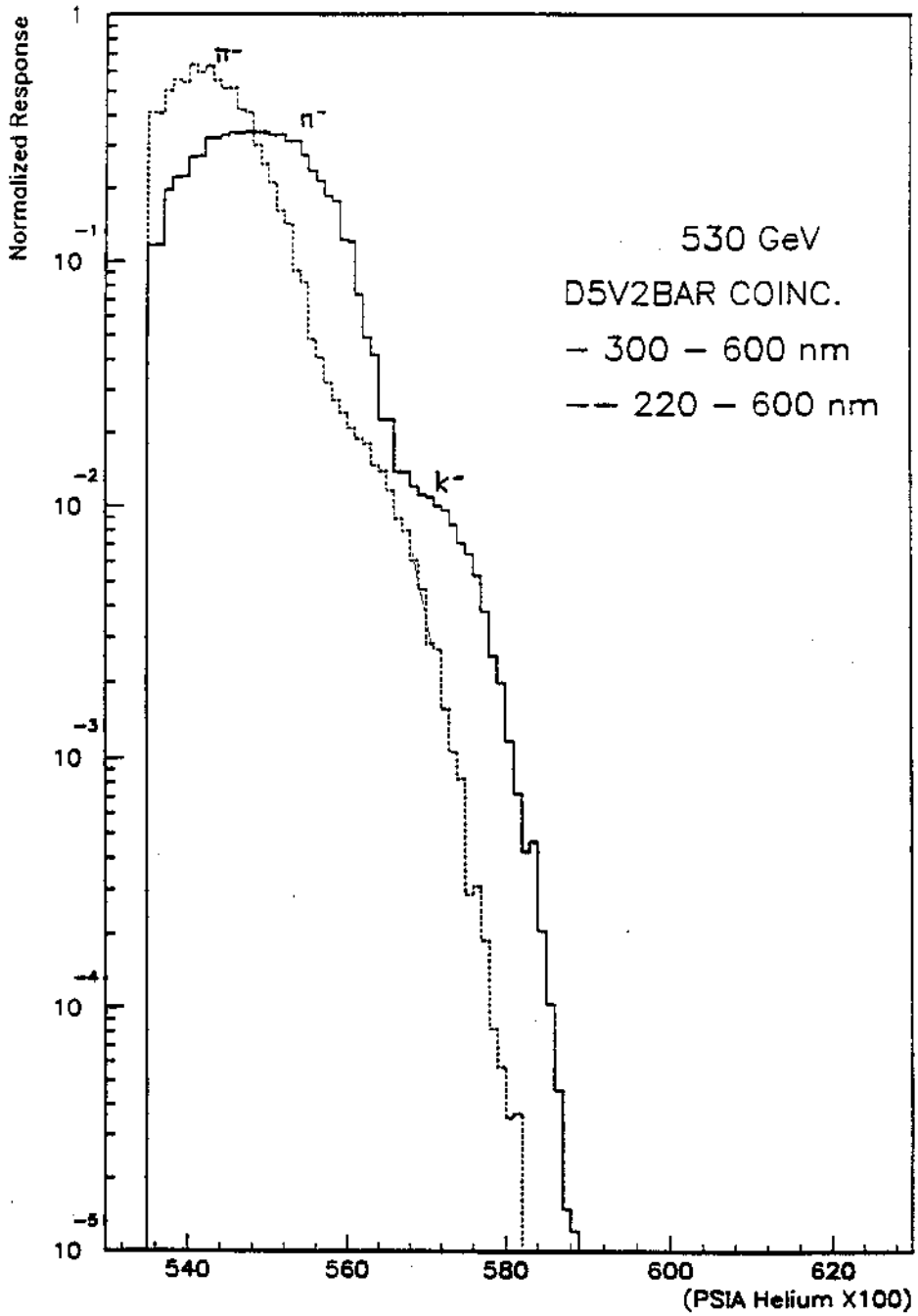

Figure 48: Effect of the accepted wavelength range on the resolution of the Cherenkov counter at -530 GeV. (top): 220-600 nm. (bottom): 300-600 nm.(97% πs and 3% Ks)

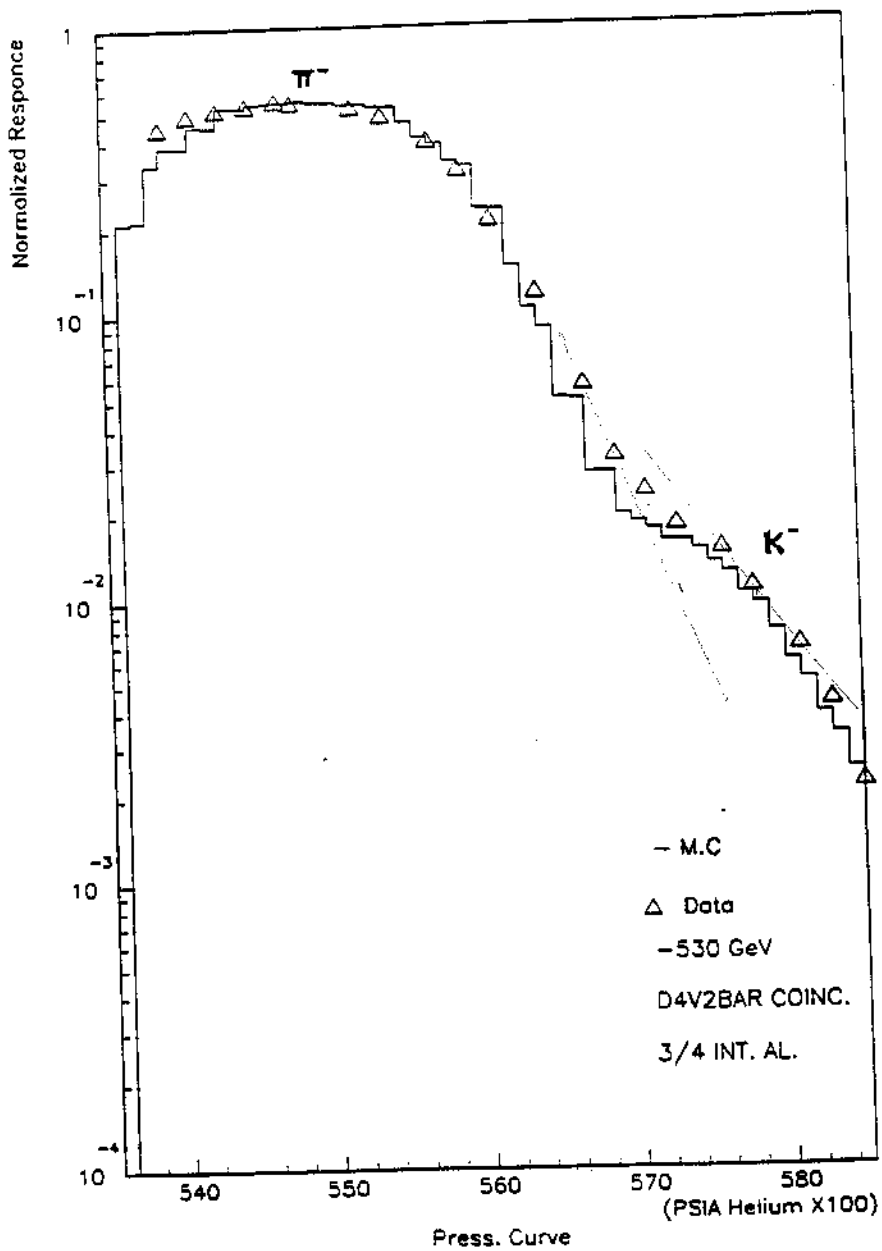

Figure 49: Comparison of the Monte Carlo pressure curve to the experimental data one at -530 GeV for the 3/4 interaction length Al target and the $D4\overline{V2}$ coincidence level.

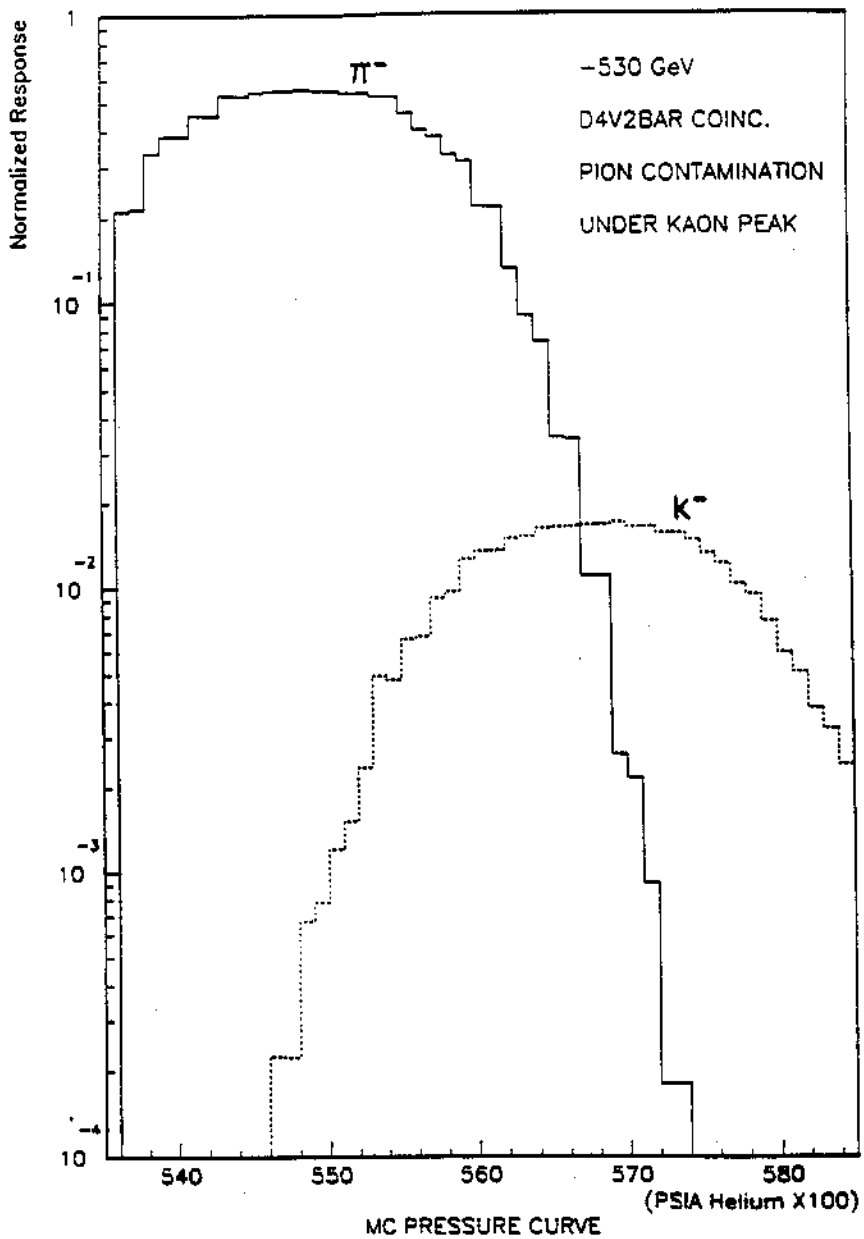

Figure 50: π^- contamination under the K^- peak at -530 GeV for the 3/4 interaction Al target and the $D4\overline{V2}$ coincidence level.

requirement (Fig. 47). The composition was determined to be: $(2.90 \pm 0.2)\%$ K^-, $(96.9 \pm 0.2)\%$ π^-, $(0.20 \pm 0.01)\%$ $\bar{p}$(the percentage of electrons and muons is on the order of 1%). The Monte Carlo with the fixed particle ratios and beam parameters was then used to to estimate the contamination to the K^-s due to the π^-s at the operating pressure point for the $D4\overline{V2}$ coincidence level (Fig. 50). The experimental $D4\overline{V2}$ pressure curve with the Monte Carlo curve superimposed on it is shown in Fig. 49. Since there were two negative runs, and the pressure points where the counter was set were not exactly the same (mainly due to different temperatures), the percentage of the beam tagged as K^- and the contaminations were run dependent.

For the first negative run (16-25 Jan. 1988), the Cherenkov counter was 58% efficient using the $D4\overline{V2}$ coincidence requirement, and 1.20% of the beam particles were tagged as K^- with less than 0.5% contamination due to π^- (less than 0.5% of the 1.20% tagged as K^- were π^- as was determined by Monte Carlo). For the second negative run (9-14 Feb. 1988), the Cherenkov efficiency was the same and 1.65% of the beam particles were tagged as K^- with less than 5% contamination due to π^-. In both runs everything that was not tagged as a K^- was called a π^-. The contamination of the π^-s by K^-s was less than 1%.

4.4.3 Positive Beam Tagging

The positive 530 GeV beam was composed mostly of protons ($\sim$ 90%), some π^+ ($\sim$ 7%) and a few K^+ ($\sim$ 1.5%). In this case, it was not possible to use

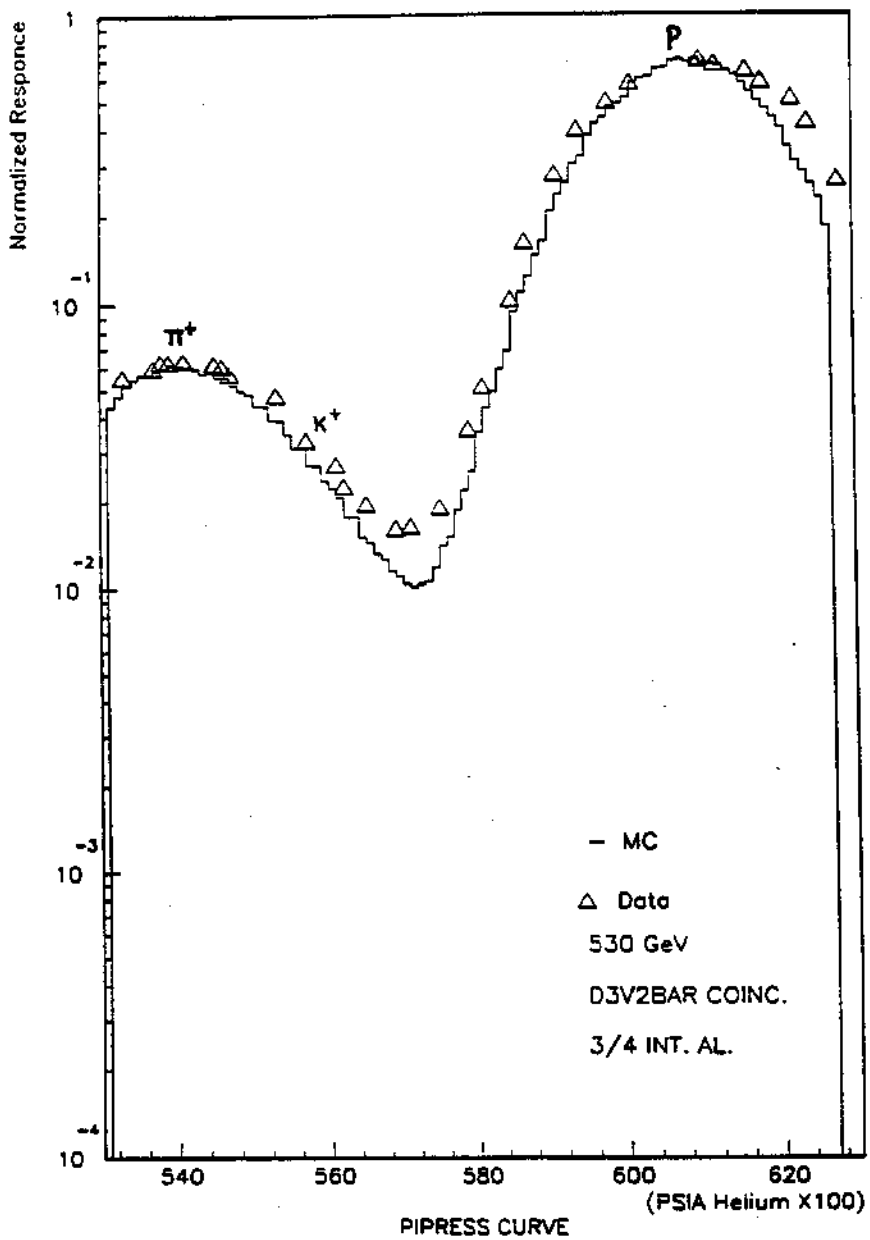

Figure 51: Comparison of the Monte Carlo pressure curve to the experimental data one at 530 GeV for the 3/4 interaction length Al target and the $D3\overline{V2}$ coincidence level.

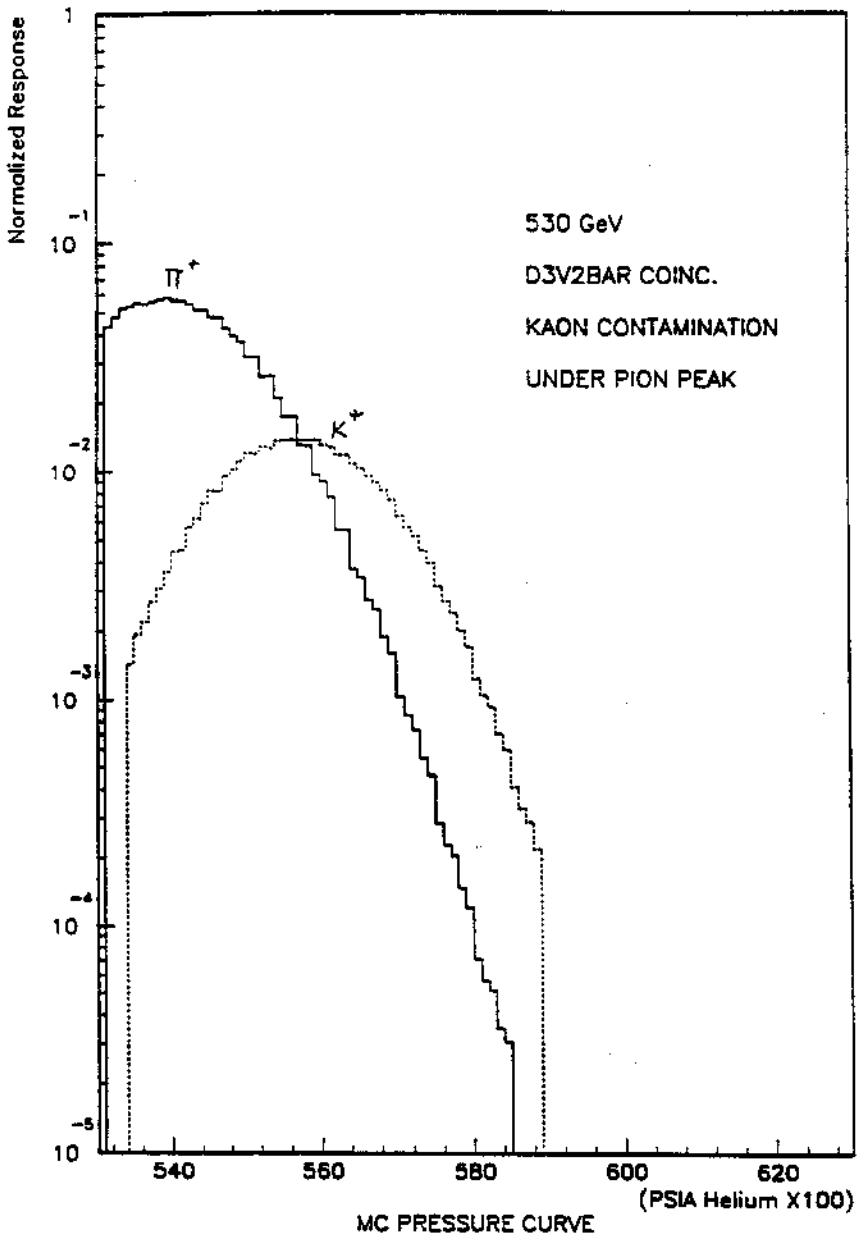

Figure 52: K^+ contamination under the π^+ peak at 530 GeV for the 3/4 int. length Al target and the $D3\overline{V2}$ coincidence level.

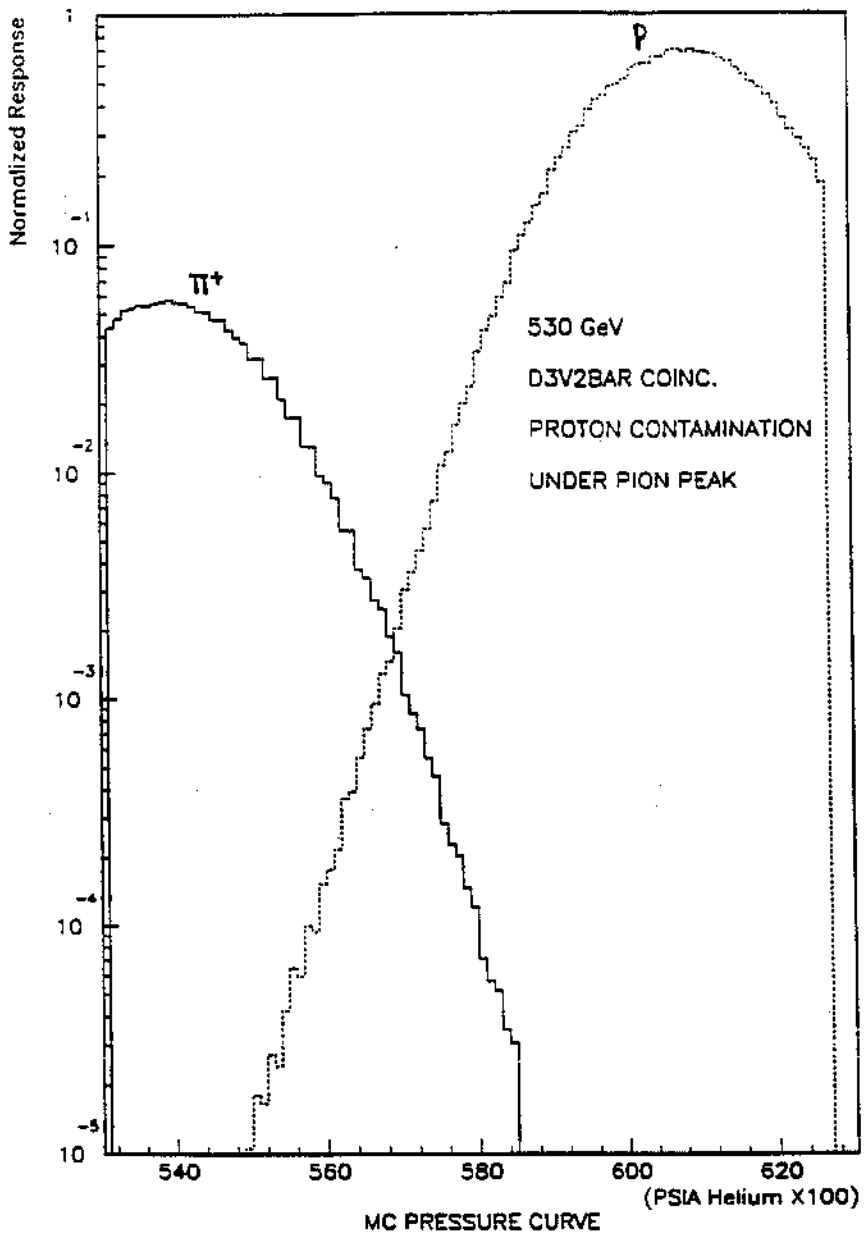

Figure 53: p contamination under the π^+ peak at 530 GeV for the 3/4 int. Al target and the $D3\overline{V2}$ coincidence level.

the Cherenkov counter to tag kaons as in the case of the negative beam, unless we wanted to have a dedicated kaon run because both the proton and pion fluxes were large. Instead, we used the Cherenkov to tag π^-s, considering the K^-s negligible and calling all the particles that were not tagged as π^-, protons.

The Cherenkov pressure was set at the pion peak and then we selected the coincidence requirement, $D3\overline{V2}$, which had the biggest efficiency and the smallest contamination.

The composition of the positive beam was determined as before by first fitting the $D5\overline{V2}$ curve (Fig. 48). The beam population was determined to be: $(7.2 \pm 0.2)\%$ π^+, $(1.7 \pm 0.1)\%$ K^+, and $(91.2 \pm 0.1)\%$ p(The percentage of electrons and muons was smaller than 0.5%). The contamination under the π^+ peak due to K^+ for the $D3\overline{V2}$ coincidence was determined from the Monte Carlo to be about 8%, while the contamination due to protons was negligible (Fig. 52 ,53). The experimental $D3\overline{V2}$ pressure curve with the Monte Carlo curve superimposed on it is shown in Fig. 51.

At the $D3\overline{V2}$ coincidence level we were 78.0% efficient and $(6.3 \pm 0.1)\%$ of the beam was tagged as π^+ with 8.0% contamination due to K^+. So the measured fraction of π^+s in the beam is:

$$\pi^+\% = \frac{(6.3 - 6.3 \times 0.08)}{0.78}\% = (7.4 \pm 0.1)\% \qquad (4.37)$$